

OPTIMAL PATH PLANNING, IMPLEMENTATION AND SIMULATION

FOR A BREAST BIOPSY SYSTEM

By

SRIDHAR RAJARAM

Presented to the Faculty of the Graduate School of

The University of Texas at Arlington in Partial Fulfillment

of the Requirements

for the Degree of

MASTER OF SCIENCE IN ELECTRICAL ENGINEERING

THE UNIVERSITY OF TEXAS AT ARLINGTON

December 2011

Copyright © by Sridhar Rajaram 2011

All Rights Reserved

## ACKNOWLEDGEMENTS

I would like to express my deep and sincere gratitude to my supervisor Dr Venkat Devarajan, PhD, Professor, Department of Electrical Engineering, The University of Texas at Arlington, for his continuous guidance and support throughout this work.

I would also like to express my thanks to Dr Ovidiu Daescu, Assistant Department Head and Associate Professor, The University of Texas at Dallas whose mathematical work is the basis of the simulation described in this thesis. I would also like to express my thanks to Dr Balakrishnan Prabhakaran, Professor, The University of Texas at Dallas, for his collaboration in this project and his team members Mr. Suraj Raghuraman, who helped me with many aspects of this thesis.

I would like to thank Dr Alan Davis and Dr Steven Gibbs for accepting my invitation to be my thesis defense.

I would like to thank my lab members and friends who offered me help and guidance during some difficult times.

Above all, I would like to express my gratitude to my parents and family members who have supported and encouraged me all my life.

November 14, 2011

## ABSTRACT

### OPTIMAL PATH PLANNING, IMPLEMENTATION AND SIMULATION FOR A BREAST BIOPSY SYSTEM

Sridhar Rajaram, M.S.

The University of Texas at Arlington, 2011

Supervising Professor: Venkat Devarajan

Core needle biopsy is a non-invasive method of confirming the presence of cancer cells in the breast. Image guided breast biopsy is a procedure performed to extract suspicious tissue and test it under the microscope for cancer. Common imaging modalities used are X-ray, MRI and Ultrasound. X-rays and MRI involve ionizing radiation which is harmful when a patient is suspected to have cancer. Apart from this, patients go through much discomfort during biopsy. Sometimes, multiple incisions are required to extract the desired tissue which prolongs the discomfort.

This thesis describes a breast biopsy system using Ultrasound images. The main aim of this system is to improve the accuracy of biopsy and also provide patients with maximum comfort. As a specific and original part of this thesis, a recently published 3D path planning algorithm, which is an important part of our overall system, is modified to fit our problem and simulated.

The path planning has been simulated for different scenarios like global minimum path, path parallel to the chest wall (rib cage), and also a path where the doctor can specify the entry region that he prefers. Results for simulation have been provided as screenshots along with a 3D projection to help view the path.

## TABLE OF CONTENTS

|   |      |
|---|------|
| ACKNOWLEDGEMENTS .....                              | iii  |
| ABSTRACT .....                                      | iv   |
| LIST OF ILLUSTRATIONS.....                          | ix   |
| LIST OF TABLES .....                                | xi   |
| Chapter   | Page |
| 1. INTRODUCTION.....                                | 1    |
| 1.1 Breast Cancer Facts .....                       | 1    |
| 1.2 Breast Biopsy Techniques .....                  | 2    |
| 1.2.1 Fine Needle Aspiration.....                   | 2    |
| 1.2.2 Core biopsy .....                             | 3    |
| 1.3 Disadvantages of Current Biopsy Techniques..... | 4    |
| 1.4 Research Motivation .....                       | 5    |
| 1.5 Specific Problem Statement.....                 | 5    |
| 2. SYSTEM OVERVIEW AND DESIGN.....                  | 7    |
| 2.1 Previous Work.....                              | 7    |
| 2.2 Redesigned ViHAB System .....                   | 9    |
| 2.1.1 Biopsy Planning Phase/Initial Setup .....     | 9    |
| 2.1.2 Biopsy Phase .....                            | 10   |
| 2.3 Components of redesigned ViHAB .....            | 11   |
| 2.3.1 Visual Imaging.....                           | 11   |
| 2.3.2 Path Planning .....                           | 12   |
| 2.3.3 Needle Tracking .....                         | 13   |

|   |    |
|---|----|
| 2.3.4 Deformation Tracking.....   | 14 |
| 2.4 Design Flowchart .....  | 15 |
| 2.5 Visual Interface.....   | 16 |
| 2.6 Advantages of Design .....  | 16 |
| 3. PATH PLANNING FOR BREAST BIOPSY SYSTEM.....  | 18 |
| 3.1 Previous Work .....   | 18 |
| 3.2 Contribution in this Thesis.....  | 23 |
| 3.3 Algorithm and Simulation .....  | 23 |
| 3.3.1 Image Acquisition.....  | 23 |
| 3.3.2 Image Segmentation .....  | 24 |
| 3.3.3 Non-Linear Anisotropic Diffusion Filter .....   | 25 |
| 3.3.4 Contour Formation .....   | 27 |
| 3.3.5 Implementing Zones of Exclusion .....   | 28 |
| 3.3.6 Target .....  | 28 |
| 3.3.7 Path Planning .....   | 29 |
| 3.3.8 An Additional Note on Computational Efficiency .....                                    | 31 |
| 3.3.9 Simulation .....  | 32 |
| 4. USER INTERFACE AND RESULTS.....  | 37 |
| 4.1 User Interface.....   | 37 |
| 4.2 Visualization .....   | 38 |
| 4.3 Results .....   | 39 |
| 4.3.1 Global Minimum Path with Zones of Exclusion.....  | 39 |
| 4.3.2 Restricted Global Minimum Path<br>With Zones of Exclusion.....                          | 42 |
| 4.3.3 Parallel Minimum Path with Zones of Exclusion<br>For different angles of insertion..... | 45 |

|  |    |
|--|----|
| 4.3.4 Selective Minimum Path with Zones of Exclusion ..... | 48 |
| 5. CONCLUSION AND FUTURE WORK.....                         | 54 |
| 5.1 Conclusion.....  | 54 |
| 5.2 Future Work.....                                       | 55 |
| REFERENCES.....  | 56 |
| BIOGRAPHICAL INFORMATION .....                             | 58 |



## LIST OF ILLUSTRATIONS

| Figure  | Page |
|---|------|
| 1.1 Fine Needle Biopsy .....  | 2    |
| 1.2 Ultrasound Guided Core Biopsy.....  | 3    |
| 1.3 Stereotactic Biopsy.....  | 4    |
| 2.1 ViHAB Block Diagram .....   | 9    |
| 2.2 Flowchart of the redesigned ViHAB system.....   | 15   |
| 2.3 Sample Visualization Interface.....   | 16   |
| 3.1 Potential Field Gradient directions with Obstacles.....   | 18   |
| 3.2 N free paths are generated, lowest cost path P' is chosen in right.....   | 20   |
| 3.3 Illustrating the Problems (a) Line hits the target<br>(b) Line penetrates target.....                             | 21   |
| 3.4 Visibility Complex (a) Hourglass corresponding to set of rays<br>(b) Transformation into Visibility Problem ..... | 22   |
| 3.5 A link L and its corresponding dual cell.....   | 23   |
| 3.6 Slice of an Ultrasound Image.....   | 24   |
| 3.7 Effect of increasing m on Diffusivity and Flux .....  | 26   |
| 3.8 Effects of non-linear anisotropic diffusion in (a) First slice (b) 167 <sup>th</sup> Slice .....                  | 27   |
| 3.9 A contour for 8-bit quantization .....  | 27   |
| 3.10 Graphical User Interface (GUI) for Restricted Global Minimum Path .....  | 33   |
| 3.11 GUI for Parallel Minimum Path.....   | 34   |
| 3.12 Projections for the different faces of the 3D Ultrasound .....   | 35   |
| 3.13 Ultrasound views of the different faces .....  | 36   |
| 4.1 User interface .....  | 38   |

|  |    |
|--|----|
| 4.2 User interface for global minimum path .....   | 40 |
| 4.3 3D projection of global minimum path.....  | 41 |
| 4.4 2D projection of paths onto first Ultrasound slice for Global Minimum path .....                 | 42 |
| 4.5 User interface for Restrictive Global Minimum path.....  | 43 |
| 4.6 3D projections of possible paths in Restrictive Global Method.....                               | 44 |
| 4.7 Projection of paths in Restrictive Global Method .....   | 45 |
| 4.8 User interface for Parallel Minimum path .....   | 46 |
| 4.9 3D projections of possible paths for Parallel Minimum path .....                                 | 47 |
| 4.10 Projection of all possible paths onto first Ultrasound<br>slice for Parallel Minimum path ..... | 48 |
| 4.11 User Interface for Selective Minimum Path.....  | 49 |
| 4.12 Selecting Quadrilateral from Ultrasound Image .....   | 50 |
| 4.13 3D projections of all paths in Selective Minimum Path Method .....                              | 51 |
| 4.14 Projection onto first Ultrasound Slice for Selective Minimum Path .....                         | 52 |

## LIST OF TABLES

| Table  | Page |
|--|------|
| 4.1 Comparison of running time and least cost for different quantization levels and threshold values ..... | 53   |

CHAPTER 1  
INTRODUCTION

1.1 Breast Cancer Facts

Besides skin cancer, breast cancer is the most commonly diagnosed cancer among U.S. women. More than 1 in 4 cancers in women (about 28%) are breast cancer. The chance of developing invasive breast cancer at some time in a woman's life is a little less than 1 in 8 (12%). Breast cancer is the second leading cause of cancer death in women, exceeded only by lung cancer. The chance that breast cancer will be responsible for a woman's death is about 1 in 36 (about 3%). In 2011, an estimated 230,480 new cases of invasive breast cancer were expected to be diagnosed in women in the U.S., along with 54,010 new cases of non-invasive (in situ) breast cancer. About 39,520 women in the U.S. were expected to die in 2011 from breast cancer, though death rates have been decreasing since 1990. These decreases are thought to be the result of treatment advances, earlier detection through screening, and increased awareness. About 1 in 8 women in the United States (12%) will develop invasive breast cancer over the course of her lifetime [1].

For detection of breast cancer, the following steps are performed in order.

1. Breast Self Examination: It is very useful in self detecting any unnatural growth in the patient's breast.
2. Clinical Breast Exam: A clinical breast examination is a physical examination of the breast performed by a health professional. Clinical breast examinations are used along with mammograms to check women for breast cancer.
3. Mammogram: The most effective way to detect breast cancer is by mammography. Mammography uses special X-ray images to detect abnormal growths or changes in the breast tissue. If abnormality is detected, then a breast biopsy is recommended.

4. Breast Biopsy: When a breast biopsy is recommended to test for breast cancer, patients may be able to choose a minimally invasive alternative to surgery known as image-guided needle biopsy. This technique does not require open surgery. Most of the time, a radiologist performs this type of biopsy. The main objective of biopsy is to remove tissue samples from the breast that are suspected to be cancerous and test them under a microscope. The needle breast biopsy can be performed using ultrasound or stereotactic guidance.

## 1.2 Breast Biopsy Techniques

### *1.2.1 Fine Needle Aspiration (FNA)*

Fine needle aspiration is a non-surgical form of breast biopsy, in which a small needle is used to withdraw a sample of cells from the breast lump. These cells will then be examined under a microscope. The patient usually sits up while the doctor inserts a small hollow needle with a syringe to withdraw (aspirate) fluid and cells from the growth for testing. When the needle reaches the mass, the doctor suctions out a sample with the syringe. The doctor repeats this procedure several times. FNA is usually a very minor surgical procedure.

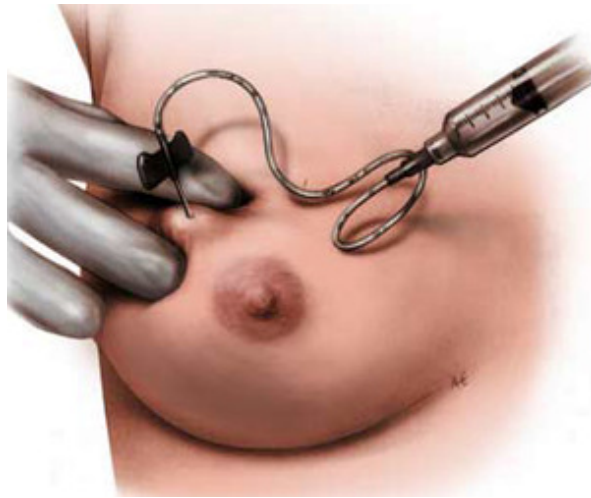


Figure 1.1 Fine Needle Biopsy

### 1.2.2 Core biopsy:

A core needle biopsy is used when your doctor needs more information about a breast lump than a mammogram, ultrasound, or fine needle aspiration can give. Core biopsy is similar to FNA, but a core biopsy uses a larger needle because actual breast tissue is removed, rather than a tiny sampling of cells. A sample of the lump is removed, but not the entire lump. The types of core biopsies include ultrasound-guided core biopsy and stereotactic biopsy.

#### 1.2.2.1 Ultrasound-guided core biopsy

This technique obtains breast tissue without surgery. A biopsy needle is placed into the breast tissue. Ultrasound helps confirm correct needle placement -- using sound waves reflected off breast tissue -- so the exact location of the abnormality is biopsied. Ultrasound can distinguish many benign lesions, such as fluid-filled cysts, from solid lesions. Tissue samples are then taken through the needle. The figure below shows the ultrasound guided core biopsy, with an ultrasound transducer and a core needle which extracts the tissue.

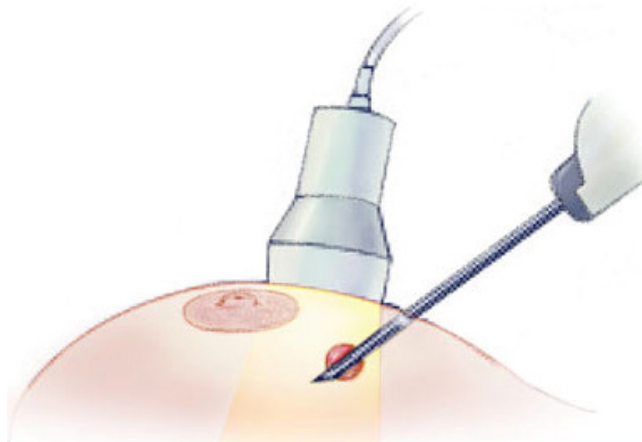


Figure1.2 Ultrasound Guided Core Biopsy

#### 1.2.2.2 Stereotactic biopsy

Stereotactic biopsy involves centering the area to be tested in the window of a specially designed instrument. Mammogram films called SCOUT films are taken so the radiologist can examine the breast tissue. Using a local anesthetic, the radiologist

makes a small opening in the skin. A sterile biopsy needle is placed into the breast tissue area to be biopsied. Computerized pictures help confirm the exact needle placement. Tissue samples are taken through the needle.



Figure 1.3 Stereotactic Biopsy

### 1.3 Disadvantages of Current Biopsy Techniques

Each method of breast biopsy has its own advantages and disadvantages. We concentrate on the combined disadvantages of the biopsy methods and try to eliminate them in a system that we have designed.

- One of the disadvantages is that other than Ultrasound guided core biopsy, other biopsies involve ionizing radiation.
- In core-needle biopsy methods, the patient is usually made to lie on her stomach. This is very uncomfortable for patients who are old or who have acid reflux.
- There is no fixed time in which a biopsy will be completed. For some patients, it takes only a few minutes, while for others it might be an hour.
- There is no fixed technique for performing biopsy. Doctors, from experience, are able to figure out how to proceed and extract the suspicious tissue. Often, the “see one do one” paradigm is unsatisfactory for training new residents.

- In some cases, multiple incisions are required to extract the exact tissue that is suspicious. This makes patients come back for multiple sittings for the biopsy to finish. It is also very painful for the patient.

#### 1.4 Research Motivation

Doctors who are performing the biopsy on patients welcomed the idea of having some guidance and visualization, while they were performing the procedure on patients. The Virtual Environment Lab (Director: Dr. Venkat Devarajan) at The University of Texas at Arlington developed a haptic guided breast biopsy training system called ViHAB. In ViHAB, the doctor guides the haptic device (to which the needle is attached) to the target cancer tissue along a guidance cone from a point on the surface of the breast to the target. The haptic device gives feedback whenever the doctor tries to deviate from this path, thereby guiding it to the tissue. While this system proved the feasibility of the approach, there were several improvements to be made. For instance, in ViHAB, the doctor would not directly manipulate the needle, but would control the needle remotely by a joystick. This did not correspond to the actual biopsy performed by interventional radiologists, who would directly insert the needle into the tissue. Thus, as a part of a new collaborative effort with Dr Balakrishnan Prabhakaran of The University of Texas at Dallas, VEL developed a newer design. This design (in consultation with interventional radiologist Dr. Kathryn Hall at Baylor Medical Center), will be able to provide doctors guidance and visualization, and also work as a training tool for novice doctors so that they will gain experience without having to perform biopsy on patients.

The imaging technique used needs to be non-ionizing, which leaves us with Ultrasound as the best option. The disadvantage with Ultrasound images is that they are noisy. We still prefer this as the imaging technique because it is a non-ionizing method.

#### 1.5 Specific Problem Statement

Currently, there is no surgical path planning algorithm in the breast biopsy system, which means that the doctor just figures out in his mind how to go and remove samples from the suspicious region. Sometimes, the doctor may need to perform multiple incisions if he does not



get the required sample, which could be very painful for the patient. There are certain zones of exclusion in the breast, which may consist of blood vessels etc, which need to be avoided during the biopsy. This could make the path planning process much more complicated. These are the two problems for which a potential solution is presented in this thesis.

## CHAPTER 2

### SYSTEM OVERVIEW AND DESIGN

#### 2.1 Previous Work

Breast biopsy has been a topic of research for many years now. There is also a new class of needles that is being developed, called bevel-tip needle which is subject to a constant turning radius upon contact with soft tissue (Alterovitz, Webster).

Yoshinobu Sato, et al., in 1998 developed an augmented reality visualization method for the guidance of breast-conservative cancer surgery using ultrasonic images (US) acquired in the operating room just before surgical resection [2]. By combining an optical three-dimensional (3-D) position sensor, the position and orientation of each ultrasonic cross section are precisely measured to reconstruct geometrically accurate 3-D tumor models from the acquired ultrasonic image.

Frank Sauer, et al., of Siemens Corporation in 2003 developed a system for augmented reality visualization of ultrasound images [3]. In this system, the user wears a custom video-see-through head-mounted display (HMD). Two color video cameras attached to the HMD provide a stereo view of the scene. A third head-mounted video camera is added for tracking. A set of markers is attached to the ultrasound transducer; a set of stationary markers can be positioned above the workspace.

Michael Rosenthal, et al., in 2002 performed randomized, controlled trials to compare the accuracy of standard ultrasound-guided needle biopsy to biopsies performed using a 3D Augmented Reality guidance system [4]. A repeated measures analysis of variance indicated that the head-mounted display method led to a statistically smaller mean deviation from the desired target than did the standard display method (2.48 mm for control versus 1.62 mm for augmented reality,  $p < 0.02$ ).

**A. Fenster, K.J.M Surry, G.R Mills and D.B Downey in 2003** developed a 3D US-guided biopsy system to integrate with Stereotactic Mammography (SM) [5]. The dual modality breast biopsy system combines the advantages of both approaches with 3D US and SM targeting, near real-time 3D and real-time 2D US guidance, breast stabilization and a confined needle trajectory. Using breast phantoms (simulated breasts using animal organs, gels, polyurethane cover materials etc.), they have shown that their ultrasound guided biopsy system was capable of targeting artificial lesions that were 3.2 mm in diameter, with a 96% success rate.

The thesis by Sumit Tandon (Dr Venkat Devarajan and Dr. Edmond Richer – co-advisors) in 2007 proposed a design of an accurate breast biopsy system, which is capable of reading and displaying three dimensional ultrasound images, keeping track of micro-calcification in near real time in a sequence of images and providing haptic guidance to a virtual needle via a force feedback joystick (figure 2.1) [6].

The imaging system was assumed to provide real time (5-10 frames per second) true 3D ultrasound images of the breast. The images would then be used to extract information, which would assist the surgeon in maneuvering the biopsy needle towards the target micro-calcification. The system could be divided into two broad parts – offline processing or the initial non-real time setup and the continuous real time operation. The first thing that the surgeon would need to do would be to view and identify the calcification. Three orthogonal slices of the ultrasound image would then be displayed on the screen. Further, localizing the calcification in 3D space would require accurate calibration of the biopsy setup and the imaging system. This would constitute the non-real time preparation for biopsy.

With the system setup and ready for biopsy, it would start operating in real time mode. In this mode, it would receive images at 5-10 frames per second and keep track of the target identified by the surgeon. It would also provide guidance to the surgeon inserting the needle by displaying a 3D model of the breast and targeted tissue. Since breast tissue is very soft, it is impossible to use the actual resistance provided by it for guidance. Hence, an amplified synthetic force

feedback was used. As the surgeon maneuvers a joystick-controlled robotic needle, real time information of the location of the target and the needle would be used to check if the surgeon was moving in the correct direction. In case the surgeon veered from the correct path, an artificial force would be applied to the joystick to set him/her in correct direction. In other words, the system would provide an “invisible haptic tunnel” to guide the surgeon. The synergy between the visual guidance and the haptic guidance, will allow the surgeon to perform a biopsy with increased accuracy, in a single attempt, without compressing the breast.

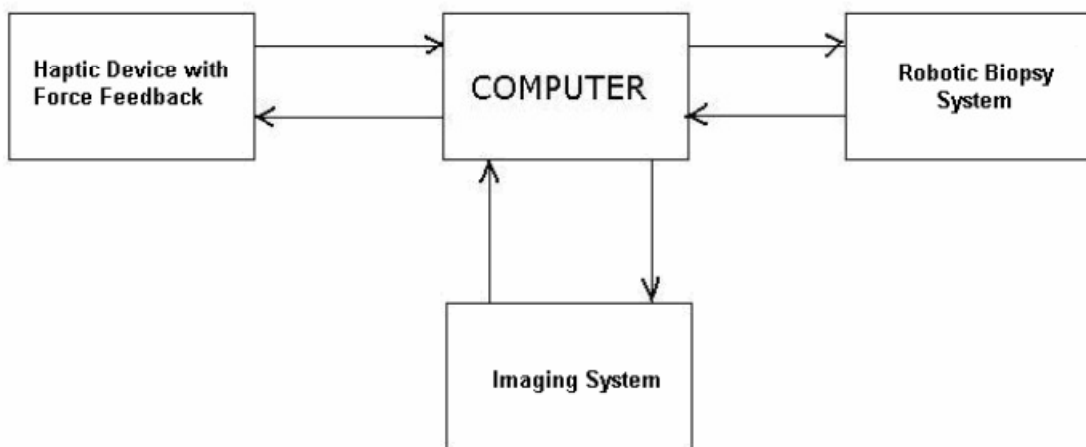


Figure 2.1 ViHAB Block Diagram

### 2.2 Redesigned ViHAB System

We at the Virtual Environment Laboratory (VEL), in collaboration with Dr Balakrishnan Prabhakaran at The University of Texas at Dallas, redesigned the ViHAB system in order to overcome some of the disadvantages that it had. The overall system can be divided into the following blocks:

1. Biopsy Planning Phase / Initial Setup
2. Biopsy Phase

#### *2.2.1 Biopsy Planning Phase / Initial Setup*

The biopsy planning phase is also referred to as the initial setup phase where we prepare the doctor and the patient for the biopsy. The patient is made to sit in a comfortable position on a chair with the surgeon sitting beside her with the ultrasound equipment on the

other side. Initially, the doctor takes a 3D Color Doppler Ultrasound scan of the breast. From the scan, he marks the target and the zones of exclusion. This is possible from the Color Doppler ultrasound scans. Cancer cells are identified mainly by the blood rings that form around them. The Color Doppler scans pick up these locations of blood (movement) and show them in a color that depends on the velocity. Once these are marked, a mesh of the entire breast is constructed from then ultrasound data, which is used for deformation tracking. Meanwhile, the 3D ultrasound images are read and the best path from the surface of the breast to the target is determined. The path is characterized by the entry point and this is shown on a display, where the doctor can use a haptic device to view it from any angle he desires.

### *2.2.2 Biopsy Phase*

This part of the biopsy is a real time process. Once the path is planned for the doctor by the system, and the deformation tracking and needle tracking systems are initiated, the biopsy is started. The doctor inserts the needle and constantly observes on the user interface the current position of the needle, target and whether he is on course to hit the target and extract the sample. The deformation tracking system helps in tracking the position of the target in real time. The needle tracking algorithm returns coordinates of the needle tip position in real time. Based on these two inputs, the user interface is made to display this information. In addition, this information is also given to the path planning algorithm in order to verify if the path needs to be modified. At this time, the constraints of the path planning algorithm will change and a new path to the target will be updated to the system and the user interface as well.

While this system proved the feasibility of the approach, there were several improvements to be made. For instance, in ViHAB, the doctor would not directly manipulate the needle, but would control the needle remotely by a joystick. This did not correspond to the actual biopsy performed by interventional radiologists, who would directly insert the needle into the tissue. Thus, as a part of a new collaborative effort with Dr Balakrishnan Prabhakaran of The University of Texas at Dallas, the Virtual Environment Lab at UTA (Dr. Venkat Devarajan – Director) developed a newer design. This design (in consultation with interventional radiologist Dr.

Kathryn Hall at Baylor Medical Center), will be able to provide doctors guidance and visualization, and also work as a training tool for novice doctors so that they will gain experience without having to perform biopsy on patients.

### 2.3 Components of Redesigned ViHAB

In the system design, we have four important components which essentially constitute parts of both the non-real time and real time processes. They are:

1. Visual Imaging
2. Path Planning
3. Needle Tracking
4. Tissue Deformation

#### *2.3.1 Visual Imaging*

We have chosen Ultrasound imaging as the imaging technique for the following reasons:

- It is a completely non-ionizing method of obtaining images, which is very important for cancer detection, because exposure to ionizing radiation for long periods is believed to help the cancer grow.
- Ultrasounds are capable of producing 3D images at real time.

The main disadvantage of Ultrasound is that the resolution of the image is poor compared to MRI or X-ray imaging. But the fact that it is capable of obtaining 3D images at real-time without using ionizing radiation is the main reason for it being used in cancer treatment.

The ultrasound image is created from sound waves in three steps - producing a sound wave, receiving echoes, and interpreting those echoes. A sound wave is typically produced by a piezoelectric transducer encased in a housing which can take a number of forms. Strong, short electrical pulses from the ultrasound machine make the transducer ring at the desired frequency. The frequencies can be anywhere between 2 and 18 MHz. The sound is focused either by the shape of the transducer, a lens in front of the transducer, or a complex set of control pulses from the ultrasound scanner machine. This focusing produces an arc-shaped sound wave from the face of the transducer. The wave travels into the body and comes into

focus at a desired depth. The return of the sound wave to the transducer results in the same process that it took to send the sound wave, except in reverse. The return sound wave vibrates the transducer; the transducer turns the vibrations into electrical pulses that travel to the ultrasonic scanner where they are processed and transformed into a digital image. At the receiver, the strength of the echo and time taken is determined and the appropriate pixel in the image is associated with a corresponding light intensity grayscale value.

Several different modes of ultrasound are used in medical imaging. We are interested only in the B, C and Doppler Color modes. In B-mode ultrasound, a linear array of transducers simultaneously scans a plane through the body that can be viewed as a two-dimensional image on screen. A C-mode image is formed in a plane normal to a B-mode image. A gate that selects data from a specific depth from an A-mode line is used; then the transducer is moved in the 2D plane to sample the entire region at this fixed depth. The color doppler makes use of the doppler effect in measuring and visualizing blood flow. Velocity information is presented as a color coded overlay on top of a B-mode image.

### *2.3.2 Path Planning*

Once the image is obtained, the next step will be in determining which path that takes us to the target with the least cost function. The breast is composed of soft tissue of varying densities. There are also blood vessels that run within the breast. Hence, we define a parameter called cost for a path which is nothing but a number which denotes which kind of tissue the path passes through. Blood vessels are given a higher value when compared to the tissue densities. This way, we will be able to arrive with a path that avoids these regions since they are very delicate and puncturing these may result in internal bleeding and other complications. The path needs to be a combination of shortest distance and least cost. Such a path is preferred over just the shortest path.

There are two stages in path planning. One is during the pre-processing step, where the initial scans are taken and after the doctor marks the target and zones of exclusion, we calculate a path per the conditions described above. Once the best path is determined, the

biopsy procedure starts. During the biopsy phase, we may need to modify the path since the zones of exclusion and the target are prone to movement due to the forces exerted during needle insertion. In real-time, the doctor will not be able to mark the target and zones of exclusion at every step. This is where the deformation tracking step is used. In deformation tracking, we propose the use of Lukas-Kanade optical flow method to continuously estimate the position of the target and zones of exclusion without the help of any further ultrasound data. Based on this information, the path may need to be changed depending on the new position of the target.

In path planning during the biopsy procedure, we need to update the path based on this information: the current position of the tip of the needle, the needle orientation and also the position of the target. Based on this information, we consider the tip of the needle to be the entry point, the new position of the target to be a new target and the orientation of the needle is very important. Based on this information, we give the doctor a series of steps to be followed to modify the path and display the new path so that the doctor can change direction and go towards the target.

### *2.3.3 Needle Tracking*

Once the path is laid out, the doctor performs the biopsy. Meanwhile, we need to monitor where exactly the needle is within the breast. This, along with deformation tracking gives us real-time updates as to where the needle is (see companion thesis by Ms. Nidhi Khullar [7]) and a predictive location of the target based on the forces generated by the needle in the direction in which it is inserted. Based on this, we can estimate whether the current path leads us to the target or not. Depending on this, we can decide whether the path needs to be modified in real time. Many of the needles tracking algorithms are based on 3D Hough transform.

The Hough transform is a feature extraction technique used in image analysis, computer vision, and digital image processing. The purpose of the technique is to find imperfect instances of objects within a certain class of shapes by a voting procedure. This voting procedure is carried



out in a parameter space, from which object candidates are obtained as local maxima in a so-called accumulator space that is explicitly constructed by the algorithm for computing the Hough transform. In other words, we look at each edge point in the image and make it vote for all the lines that it could possibly lie on. Finally the line that gets the most votes is returned.

Another important role of needle tracking is to determine the angle at which the needle is inserted. This is a very important aspect when we change the path when the target has moved due to some reason.

#### *2.3.4 Deformation Tracking*

Tissue deformation is the process of predicting the movement of the tissue within the breast upon insertion of the needle. Since the breast is composed of soft tissues of varying densities, they are subjected to some sort of movement when a needle is inserted into it for example. The movement may be very small, but considering the size of the micro calcification, this movement could result in large error when tissue sample is extracted for biopsy procedure. We use the Optical flow method of deformation tracking developed by Lukas-Kanade for this system. The reason is less sensitive to image noise than point-wise methods. This is justified by the fact that among all imaging modalities, Ultrasound imaging has the most noise. The Lukas-Kanade method assumes that the flow is essentially constant in a local neighborhood of the pixel under consideration, and solves the basic optical flow equations for all the pixels in that neighborhood, by the least squares criterion.

A flowchart of the working of the overall system is given below.

## 2.4 Design Flowchart

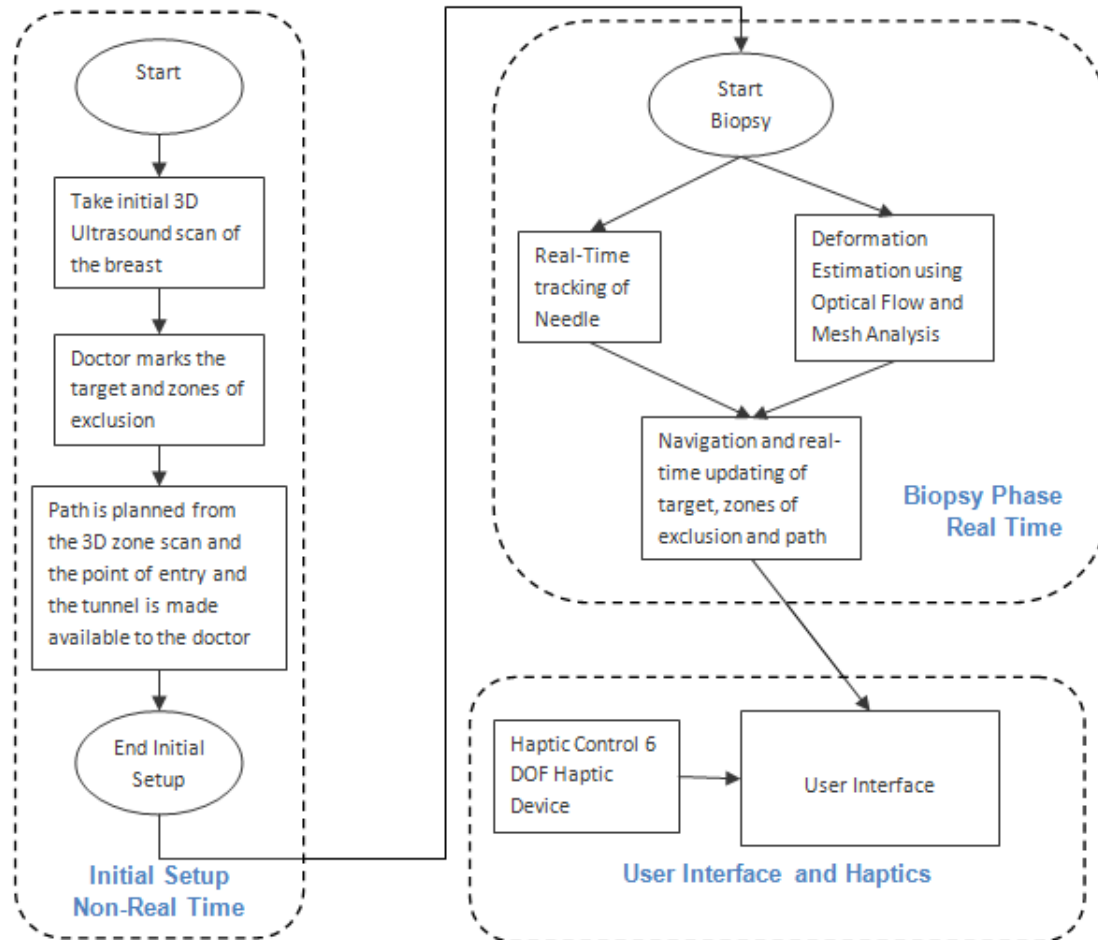


Figure 2.2 Flowchart of the redesigned ViHAB system

## 2.5 Visual User Interface

A sample interface, which the doctor will be able to see while performing the biopsy, is shown in figure 2.3. The red dot shows the target and the yellow region highlights the path that is to be followed.

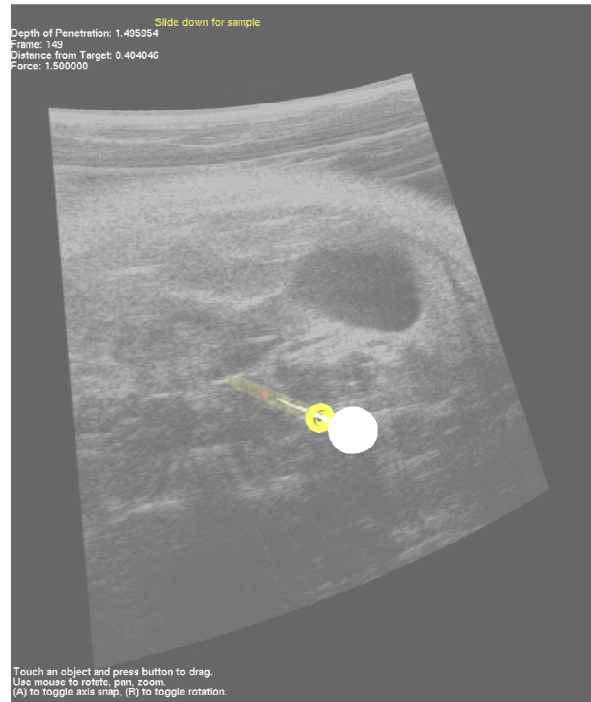


Figure 2.3 Sample Visualization Interface [8]

The path will be displayed based on the optimal entry that is returned by the path planning algorithm. The visualization module has an input which is the needle tracking block, to show where the tip of the needle is. This will be connected to a 6 degree of freedom (DOF) haptic joystick, which the doctor will be able to rotate and can visualize at any angle with which he thinks he is able to get the complete picture of the biopsy.

## 2.6 Advantages of Design

The main objective of this system is to minimize the disadvantages of the previous system designs and also give the doctor freedom to perform the biopsy instead of him holding a haptic device and blindly following the force feedback path given to him.

Some of the advantages of this system are:

- The patient is made to sit on a chair and not lie on her back. This makes it very comfortable for older patients and those suffering from acidity problems.
- The deformation tracking part of the system constantly estimates the movement of the target, and hence we get real-time updates of the target. This increases the accuracy of the overall system and could potentially avoid multiple insertions and multiple sittings.
- The doctor is able to visualize the path and get real-time feedback of the position of the needle thereby improving the accuracy of the system.
- From the color doppler ultrasound scans, the blood vessels become visible and when these are taken in to account (as is done in this thesis), these also called zones of exclusion can be left undamaged during biopsy.

In this thesis, the primary focus is in the simulation of a recently published general algorithm for the path planning to our specific application of biopsy needle path planning.

## CHAPTER 3

### PATH PLANNING FOR BREAST BIOPSY SYSTEM

#### 3.1 Previous Work

This topic has been under research for over a decade now.

Simon P. DiMaio and S. E. Salcudean in 2005 developed a new concept of needle steering and a needle planning Jacobian defined using numerical needle insertion methods that include needle deflection and soft tissue deformation [9]. This concept is used in conjunction with a potential-field-based path planning technique to demonstrate needle tip placement and obstacle avoidance. They used an attractive parabolic potential well placed at the target and a repulsive parabolic well placed near the obstacles (figure 3.1). The planning was based on bevel-tip needles. The direction of the needle could be changed by rotating the needle at the base. They planned to use a step by step motion for the needle motion so that they could at each step predict the position of the target and then give step by step instructions to be performed.

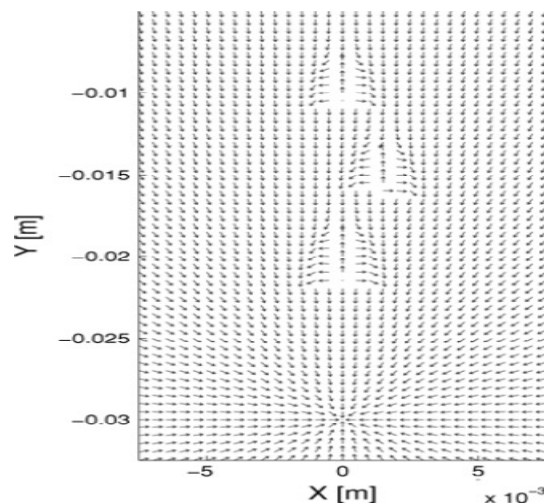


Figure 3.1 Potential Field Gradient directions with Obstacles

Ron Alterovitz, Ken Goldberg and Michael Branicky in 2009 developed a new motion planning algorithm for a variant of a Dubins car with binary left/right steering and apply it to steerable needles, a new class of flexible bevel-tip needle [10]. The planner computes optimal steering actions to maximize the probability that the needle will reach the desired target. Given a medical image with segmented obstacles and target, they formulate the planning problem as a Markov decision process. This algorithm is based on 2D imaging and improved for 3D imaging. Also, they use MRI and X-ray imaging to get high resolution data.

Ron Alterovitz, Ken Goldberg and their team from University of California Berkeley in 2009 presented algorithms for simulating and visualizing the insertion and steering of needles through deformable tissues for surgical training and planning [11]. They model the coupling between a steerable needle and deformable tissue. They introduced a novel algorithm for local remeshing that enforces the matching of a tetrahedral mesh to a curvilinear needle path, enabling accurate computation of contact forces, an efficient method for coupling a 3D finite element simulation with a 1D inextensible rod with stick-slip friction, and optimizations that reduce the computation time for physically based simulations.

Ron Alterovitz and Ken Goldberg with another team of researchers from University of North Carolina and John Hopkins University in 2009 developed a feedback controller that steers a bevel-tip needle along 3D helical paths to achieve high accuracy for targets sufficiently far from the needle insertion point [12]. They used a model predictive control framework that twists the needle such that the predicted helical trajectory minimizes the distance to the target.

Laurence Vancamberg, Anis Sahbani, Serge Muller and Guillaume Morel in 2010 developed an approach that couples path planning methods along with Finite Element Simulation in order to find an optimal path taking breast deformation into account [13]. The planning approach is in four steps: Generation of a low-cost path  $P'$  with relaxed constraints, Needle insertion simulation along  $P'$  and  $ZP'$  definition, family  $FP'$  of optimal candidate paths generation, optimal path  $P^*$  selection. The figure shows that for path estimation, they have used

Rapidly Exploring Random Trees method. They have also considered the blood vessels as part of the path and assigned a cost to each path (figure 3.2).

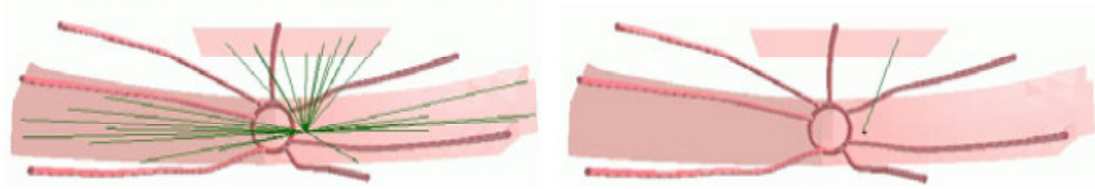


Figure 3.2 N free paths are generated, lowest cost path P' is chosen in right

Ron Alterovitz, Kenneth Y. Goldberg, Jean Pouliot and I-Chow (Joe) Hsu in 2010 developed a needle insertion motion planning system based on an interactive simulation of needle insertion in deformable tissues and numerical optimization to reduce placement error [14]. It was a 2-D physically based, dynamic simulation of needle insertion that uses a finite-element model of deformable soft tissues and models needle cutting and frictional forces along the needle shaft. Using texture mapping, the simulation provided visualization comparable to ultrasound images that the physician would see during the procedure.

The work previously described primarily involves path planning in a 2D image/space. The work in 3D has been very limited. The main background to the 3D simulation that has been done was given by Prof. Ovidiu Daescu at the University of Texas at Dallas. His two papers; one published in September 2000 and the other in August 2003, which was further revised in July 2008, constitute the main theoretical background for my thesis [15]. In the following paragraph a brief overview of the theory is given.

In his paper, he described an algorithm for determining the optimal penetration among weighted regions for 2D and 3D spaces [16]. The 3D case was not implemented but a proof of concept was presented. In the 2D case, he considered it to be one of two problems: 1) the line stops after hitting the target (figure 3.3(a)); 2) the line penetrates the target and comes out the other side (figure 3.3(b)). He used a combination of *topological sweep* and *topological walk* techniques to solve the problems. Using topological sweep, it was shown by Edelsbrunner and Guibas that if we have a set of  $n$  straight lines  $H = \{l_1, l_2, \dots, l_n\}$ , all the faces (i.e.

cells/vertices/edges) could be traversed in  $O(n^2)$  time.. Further, a portion of a convex region  $P$ , say  $A(H)$ , with  $r$  boundary vertices could be computed in  $O(K+(n+r)\log(n+r))$  time and  $(n+r)$  space using the topological walk technique.

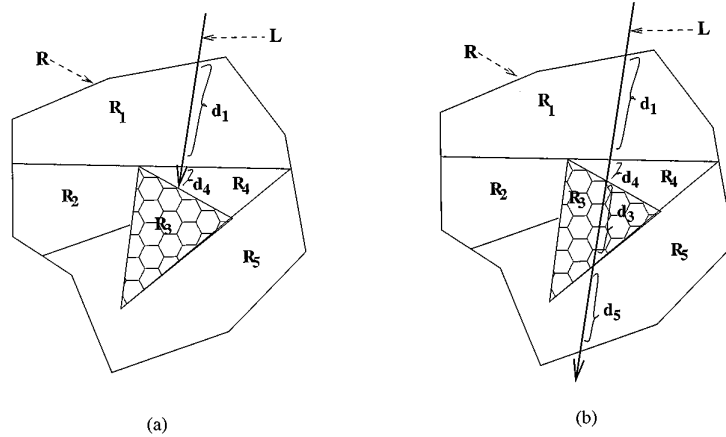


Figure 3.3 Illustrating the problems: (a) line hits the target; (b) line penetrates target

In the algorithm, he used the concept of the visibility transform, which is similar to the Hough transform. Pocchiola and Vegter [17] first introduced visibility complex as a data structure for representing collections of line segments in the object-free space of the scene that have same visibility properties. The main concept of visibility complex is to convert the lines in the spatial domain into a dual space using a duality transform, where the lines are transformed into points and the end points that bound the region are transformed into lines (figure 3.4). In the dual plane, an optimization function was used to determine the point with the least cost within each cell (a cell in the dual space is a closed region that is formed by transforming the end points in the spatial domain). When the inverse transform was applied, this optimized point is transformed into a line in the spatial domain. Thus, they arrived at a set of paths that are optimized over many regions. An optimization function in the spatial domain will then select the optimal path from the previously obtained paths.



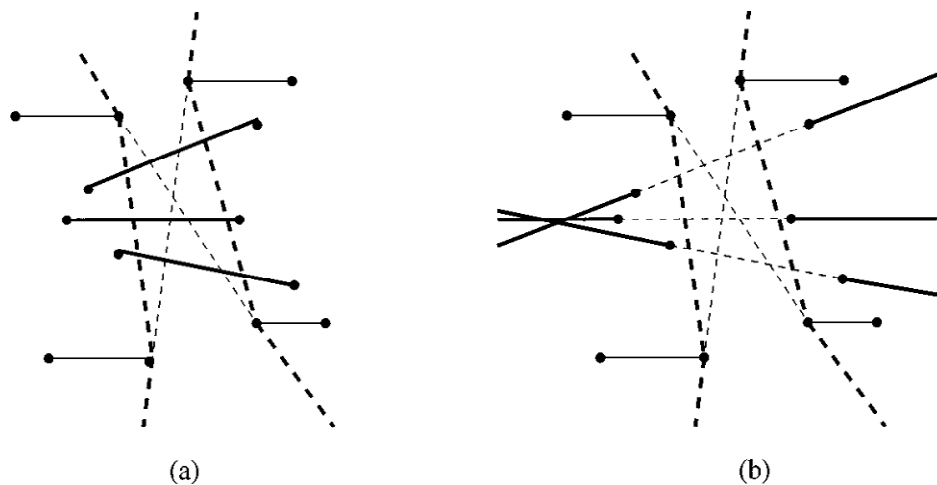


Figure 3.4 Visibility Complex (a) Hourglass corresponding to set of rays  
 (b) Transformation into Visibility Problem

In the 3D case, a line can be described by 4 parameters: two spherical coordinates  $(\theta, \phi)$  of the direction vector of the line and the projection  $(u, v)$  onto the plane orthogonal to the line containing the origin. Hence, a cell here becomes a 4-D dual space. The topological walk and topological sweep algorithms do not exist for the 4-D case. As in 2D, the visibility complex is constructed based on a direct enumeration of the vertices. The storage capacity of this is  $O(n^4)$  in the worst case, where  $n$  is the total number of edges of the polygons in the 3D space. Now a depth-first search of the 4-D visibility complex is performed in order to identify the cells of the dual plane. With each cell visited, we maintain a sequence of points in the 3-D volume that are intersected by the line in a way similar to the 2-D case. This results in a very complicated expression for the cost estimation in 4D. Instead, the line is describes as  $L_z$  and  $L_y$  being the projections of the line onto  $z = 0$  and  $y = 0$  respectively. Now, the line is expressed using parameters  $(u, v, \theta, \phi)$ , where  $u$  and  $v$  are the coordinates of the intersection point of the line with  $x = 0$ , and  $\theta$  and  $\phi$  are the slopes of  $L_z$  and  $L_y$ . As in the 2D case, we consider the domain transformation by converting the hourglass created by the intersection of the line and the weighted regions (figure 3.5(a)) into the dual plane and estimating the least cost function using

an optimization function (figure 3.6(b)). But since this is a 3D case, a different dualization is suggested.

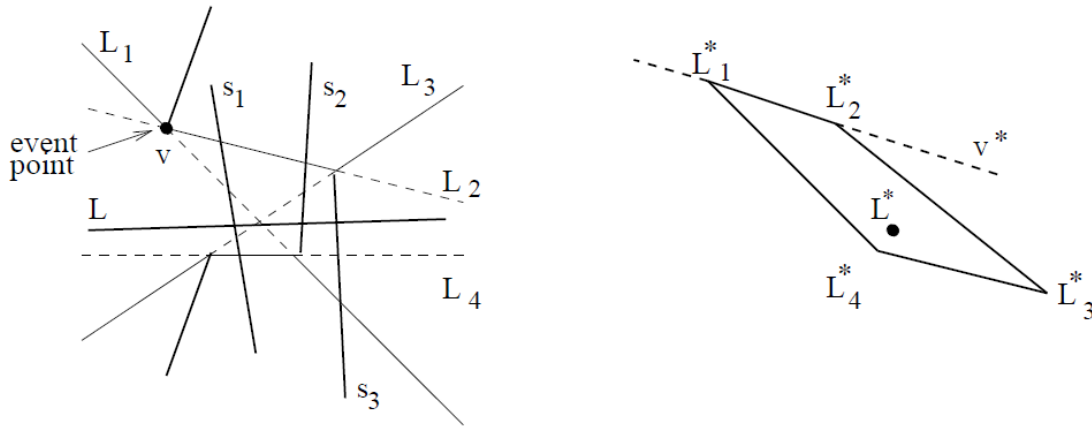


Figure 3.5 A link  $L$  and its corresponding dual cell

### 3.2 Contribution in this Thesis

In this thesis, we have used the theoretical approach suggested by Dr.Daescu, and modified it to work for ultrasound breast images. Simulation of this algorithm for various conditions is explained in greater detail later in this chapter. The results of simulation are given in the next chapter. A 3D to 2D perspective projection is used to get a better view of the paths that are generated. To get a view of how the path looks on the Ultrasound image, we have projected the paths onto the XY plane i.e. the first slice of the Ultrasound image.

### 3.3 Algorithm and Simulation

The modified algorithm is explained in this section. We have used Matlab as the tool for executing this algorithm.

#### *3.3.1 Image Acquisition*

The first step involved is to read the 3D Ultrasound data that is stored on the machine. 3D ultrasound is a data set that contains a large number of 2D planes (B-mode images). Once these images are stored by the ultrasound device, we construct them into a 3D array by placing

these slices one behind the other to create a 3D volume with a number of nodes which have a certain value assigned to them.

Figure 3.6 shows one slice of the ultrasound image which contains 512x512 pixels. The 3D array will have 216 of these images stacked one behind the other. In other words, we will have 512x512x216 pixels.

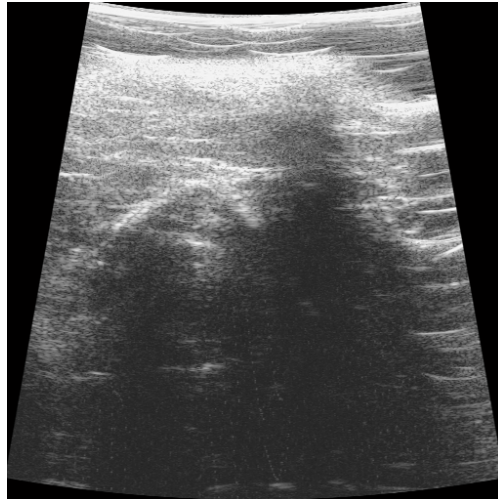


Figure 3.6 Slice of an Ultrasound Image

A Matlab code is written which fetches the Ultrasound images from a specific directory and creates a 3D array from them. The code is automated such that if we know the name of the first image, the program will be able to generate the whole array automatically, because the ultrasound device stores the images in an orderly manner.

### *3.3.2 Image Segmentation*

The main processing of the ultrasound image in order to apply the theorem, given by Dr.Daescu, is to segment the Ultrasound image. Segmentation refers to the process of partitioning a digital image into multiple parts within which some homogeneous properties are evident. The goal of segmentation is to simplify and/or change the representation of an image into something that is more meaningful and easier to analyze. Image segmentation is typically used to locate objects and boundaries (lines, curves, etc.) in images. More precisely, image

segmentation is the process of assigning a label to every pixel in an image such that pixels with the same label share certain visual characteristics.

The main aim in segmentation is to mark the boundaries between image contours. As we have mentioned before, the image pixel values are used for computing the cost of a path. For obtaining image contour boundaries, the inbuilt Matlab function returned a lot of smaller contours because of the noisy nature of the Ultrasound image. This will be algorithmically redundant and thus time consuming. We need to find a way to reduce the number of contour boundaries, eliminating the noisy boundaries and retaining the important ones.

The image needs to be blurred and then extract the image contours. A Gaussian blur was applied which resulted in blurring the edges which resulted in detection of the more prominent edges between contours. A similar result is obtained when a linear diffusion filter is used. Therefore, we used a non-linear diffusion filter.

### *3.3.3 Non-Linear Anisotropic Diffusion Filter*

Diffusion filters based on the partial differential equation are used to enhance the image quality. The diffusivity in a non-linear anisotropic filter is a tensor (consists of both a scalar magnitude and a direction vector) that varies with both the edge location and its orientation whereas it is a constant in linear diffusion filters. Therefore, diffusion across the edge can be prevented while allowing diffusion along the edge. This prevents the edge from being smoothed during the denoising.

There are four parameters which are involved in the calculation of diffusion filters: contrast parameter  $\lambda$ , speed of diffusivity  $m$ , space regularization parameter or standard deviation of the Gaussian kernel  $\sigma$ , and number of steps  $T$ .

The contrast parameter  $\lambda$  is used in the calculation of diffusivity (equation 3.1). The symbol,  $\lambda$ , plays the role of a contrast parameter separating forward (low contrast) from backward (high contrast) diffusion areas. Also, with the increase in  $\lambda$ , diffusivity increases for the same gradient. The value of  $\lambda$  used in this thesis is 3.

$$g(s) = \begin{cases} 1 & \text{for } s \leq 0 \\ 1 - \exp\left(-\frac{c_m}{\left(\frac{s}{\lambda}\right)^m}\right) & \text{for } s > 0 \end{cases} \quad (\text{equation 3.1})$$

The parameter 'm' defines the speed of diffusivity and the flux changes for a variation in the gradient. Diffusivity and flux changes quickly for larger values of m (figure 3.7). In this thesis, a value of 16 for 'm' is used.

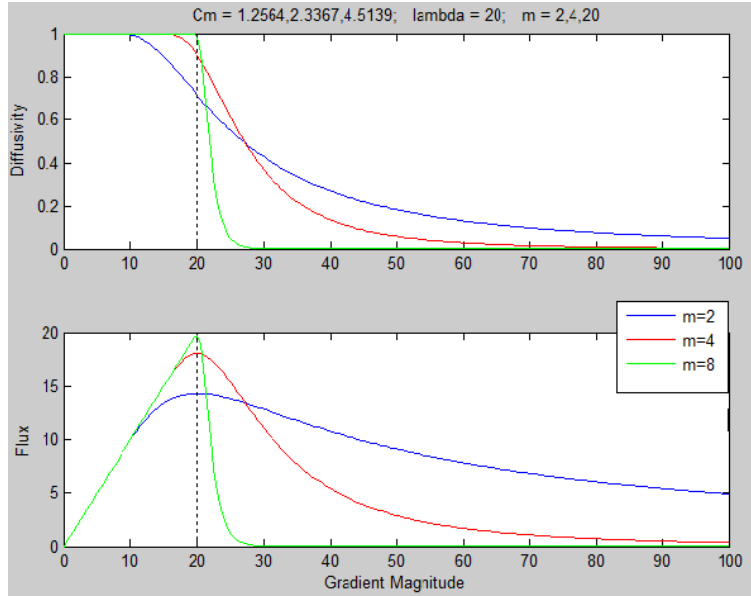


Figure 3.7 Effect of increasing m on Diffusivity and Flux

' $\sigma$ ' is the standard deviation of the Gaussian filter, which is convolved with the image before the gradient is calculated. By increasing  $\sigma$ , the Gaussian filter becomes faster and more insensitive to small-size structures. This also leads to stronger blurring of large structures and hence they become difficult to segment. For the set of images that we worked with, a value of 3.5 worked well.

Number of steps T represents the number of times the diffusion filter step is repeated. Different values of T provide a family of subsequently simplified versions of the original image, which gives a hierarchy of structures and allows extracting the relevant information from a certain scale. For our needs, we have used a T value of 20.

Figure 3.8 shows the effect of diffusion on different slices of the Ultrasound Image.

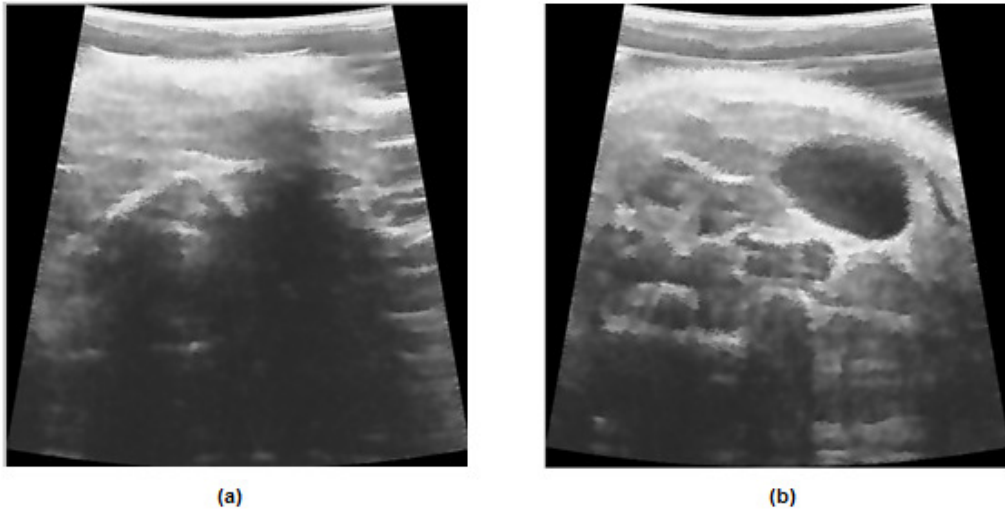


Figure 3.8 Effects of non-linear anisotropic diffusion in a) First slice b) 167<sup>th</sup> Slice

### 3.3.4 Contour Formation

Once the image is diffused, we need to segment the image and obtain the image contours. The process of grouping the image pixels into regions based on their intensity is called contouring. For this step, we first quantize the diffused image. Quantization is a lossy compression technique achieved by compressing a range of values to a single quantum value. We use 16 bit quantization for our algorithm. Once all the ultrasound slices are quantized, we identify the contours that are present in all the slices of the ultrasound image. This helps in grouping the regions of similar intensities in 3D. One such contour that is present in all the slices is shown in figure 3.9.

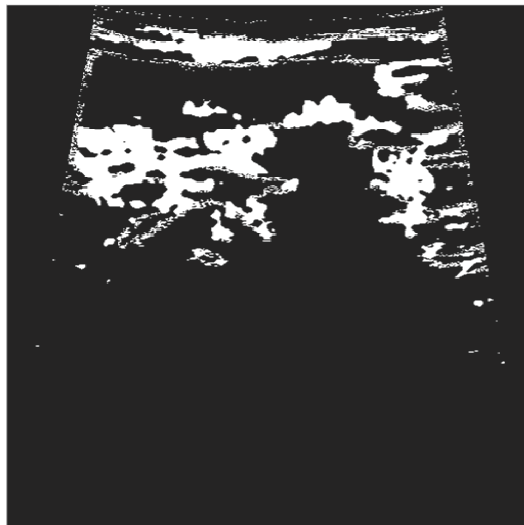


Fig. 3.9 A contour for 8-bit quantization

As we can see from the ultrasound slice, the actual ultrasound data is limited to a certain portion of the image. There will be some contours that are generated along the boundary of the ultrasound image. We eliminate these smaller contours based on a threshold and retain only the significant contours. The main aim of the algorithm is to calculate a least cost path. We consider pixel intensities of the ultrasound image to represent the tissue density. This logically implies that we need to make a lot of points lie on the same contour while calculating the path. This ensures that in the less dense regions, we will get a lot of points that lie in the same weighted region, making the cost of the path less.

### *3.3.5 Implementing Zones of Exclusion*

One of the most important aspects of path planning is to consider blood vessels (also called zones of exclusion). The zones of exclusion will ideally be marked by the doctor from the color doppler ultrasound scans. This is an improved version of an ultrasound or B-mode scan. In color doppler ultrasound, velocity information is presented as a color coded overlay on top of a B-mode image. Blood vessels carry blood and therefore they have a lot of movement within them all the time. Hence, these regions appear red in color in the doppler scan. The doctor can then mark these regions so that a higher weight will be assigned to these regions which indicate that they must be avoided during biopsy.

Since we are running a simulation, we are not generating the ultrasound images on a patient. We were given access to some already obtained ultrasound data by Dr. Mathew Lewis, Assistant Professor at The UT Southwestern Medical Center at Dallas. We have used this image to test the algorithm. Due to this fact, we are generating some random quadrilaterals/parallelepipeds and assigning an infinite weight to these regions.

### *3.3.6 Target*

In the proposed system, the doctor will mark the cancer cell that he wants to extract during biopsy in the 3D color doppler ultrasound image. To simulate that situation, a 3D point is randomly assigned within the Ultrasound image set and to be our target.

### 3.3.7 Path Planning

Now, we start the actual path planning process. In the previous work that was described, the 2D path planner was implemented. We modified that algorithm to work in 3D to suit our particular case.

The main objective of path planning is to estimate an optimal path that takes the doctor from the surface of the breast to the target that was marked by the doctor while avoiding the zones of exclusion. There is also a secondary objective to path planning; this is path updating. This happens during the biopsy process based on inputs from deformation tracking and needle tracking. We concentrate on the biopsy-planning phase, where the initial path is planned for the doctor.

To determine the path, we start from the target and retrace the line towards the entry point. We consider each contour that was common to all the faces of the ultrasound image. For each point on that contour, we construct a line from the target, passing through the point on the contour, and extend it towards the surface to determine the entry point of that particular line. This procedure is carried for points that lie on different contours on the slice before the target, on the slice containing the target and the slice that succeeds the target slice. We consider these three slices specifically because all the paths that have entry points before the target will pass through some point on the slice prior to the slice containing the target. Points on the slice of the target will constitute paths which have entry points on the same slice. The points on the slice following the target will account for all paths that have entry points behind the target slice. From the slope intercept form of a line, we know that given any 1 coordinate and the slope, we can determine the other two coordinates. Equation 3.2 describes the slope intercept formula used to calculate the points on a given line.

$$\frac{x-x_1}{x_2-x_1} = \frac{y-y_1}{y_2-y_1} = \frac{z-z_1}{z_2-z_1} \quad (\text{equation 3.2})$$

During the biopsy, we need to determine a path that takes the doctor from the surface of the breast to the target. But during the path planning process, we assume the target to be the



starting point and then retrace the path from the target to the surface of the breast through each contour point obtained. Therefore, the target is assumed to be the starting point, i.e.  $(x_1, y_1, z_1)$ . In each slice, we locate the contour point and assign the values  $(x_2, y_2, z_2)$  to it. Now, we have three unknowns; x, y and z. In order to solve the equation, we need to assume one of the three unknowns and then determine the other two coordinates from the equation given above. The preferred variable to assume will be z, because it represents the slices of the images. So, for each slice, we can determine the exact location of points that belong to that particular path. In some cases, the position of the contour points will be in such a way that they lie close to the edge of the slice right next to the target. Also, there will be contour points that lie on the slice of the target. In those cases, this method will not give the correct path. In order to fix this problem, we use the following method to assume the values for x, y or z. We assume the coordinate, which has the largest difference to be the known and increment/decrement it based on the direction of the line joining the target and the contour point.

In representative terms, we take the  $\max [abs(x_1 - x_2), abs(y_1 - y_2), abs(z_1 - z_2)]$ . We assume the variable that has the largest difference and then decrement/increment it depending on the direction from the target to the contour point. We can then estimate the values of the other two variables, thereby getting 3D coordinates for every point that lies on that path.

After the variables are determined, a feasible entry point is determined for each path such that it lies on any one of the surfaces of the ultrasound image. The entry points on the last slice of the Ultrasound image are not considered because the biopsy cannot be performed from behind. The entry point plays a very important role since it is the start of the biopsy and also it sends information to the user interface to depict the path that has been planned so that the doctor can get details of the path from any angle he wishes. The entry point is also important in deformation tracking as the forces for deformation depend on the initial point and the direction/angle at which the needle is being inserted.

Once the path is determined, we need to assign a cost function to each path. For this, we visit each point that was determined to lie on each path and then add up the intensity values in the

ultrasound image corresponding to each point to constitute a cost for a path. This is stored in the same location as the contour point. Since the cost is estimated by adding up the pixel values from the image, we can safely assume that the shorter the path, the smaller will be this cost function. Also, if the path intersects a zone of exclusion, it will have a high cost because these zones were assigned a higher value when compared to the other pixels. A logical conclusion from lowest cost path will be to arrive at a path which will cause least amount of pain during the biopsy. One way of ensuring that is to traverse the regions with least cost all the time. For this, we make sure that all the points on a particular line lie on the same contour all the time. This proves effective in certain cases, but for a lot of target positions, there is no way of reaching the target by passing through just one contour. So, we use a threshold of 75%, i.e. at least 75% of the points on a path should lie on the same region as that of the point on the contour that was considered. 75% is just a threshold that was used for the algorithm. The threshold value can be changed as per requirement (either greater accuracy or faster running time). The tradeoff is between the accuracy and running time.

### *3.3.8 An Additional Note on Computational Efficiency*

The intent of the needle path planning is to help the interventional radiologist in a timely manner to design the least painful path from the surface of the breast to the cancer cell location. While it is reasonable to request that physician locate the target cell, circle the zones of exclusion etc. on the ultrasound images, it is imperative that the algorithm provide the potential path(s) in a matter of seconds. When the real time C++ code is implemented for our algorithm, this is the scale of time that we need to design in to the system. Given that the corresponding MATLAB code can take about 20 times that time line suggests that the algorithm run on MATLAB in less than two minutes. It is clear that the chief driver of this time line is the number of possible paths that are candidates based on our decimated, hierarchical data set of contour points. Fortunately, this can be controlled by the values of threshold and quantization level.

### 3.3.9 Simulation

As a feature of this thesis, we extend this path planning algorithm to help under various scenarios.

1. For a novice doctor who has never performed a biopsy before, we will do the path planning for the entire 3D volume and return one global minimum entry point, through which biopsy is to be performed. Some doctors (Dr. Robert Wynn of UT Southwestern was one of them) with whom we had interacted said that they preferred performing the biopsy parallel to the rib cage (or chest wall). The global minimum path is restricted to have entry points only in four faces and within a specific tolerance level that the radiologist specifies (figure 3.11).

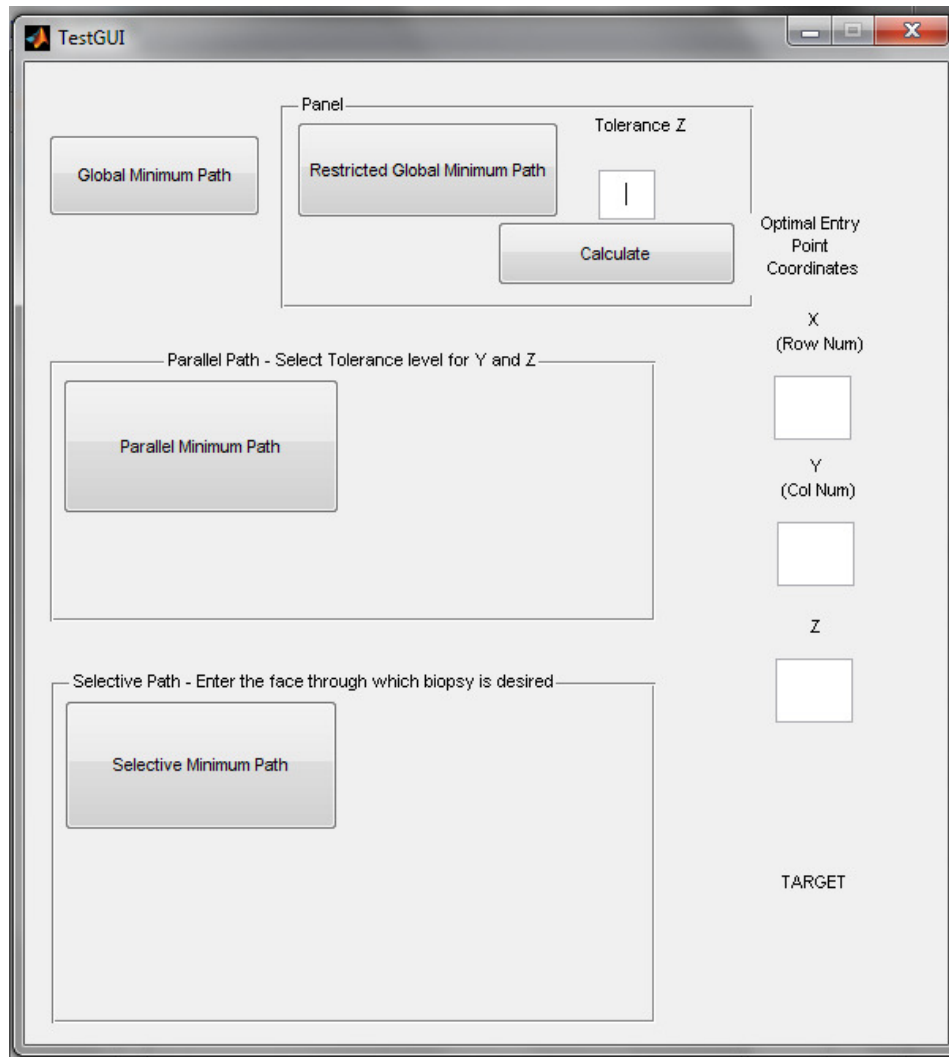


Figure 3.10 Graphical User Interface (GUI) for Restricted Global Minimum Path

We further reduce the accidental possibility of puncturing the lung by totally eliminating 2 more faces as candidate entry points, and limit the angle of insertion in another dimension, which makes the path parallel to the chest wall, with some tolerance given to the angle of insertion. For this type of path planning, the doctor needs to provide inputs in the form of a tolerance level in the Y and Z directions (figure 3.12).

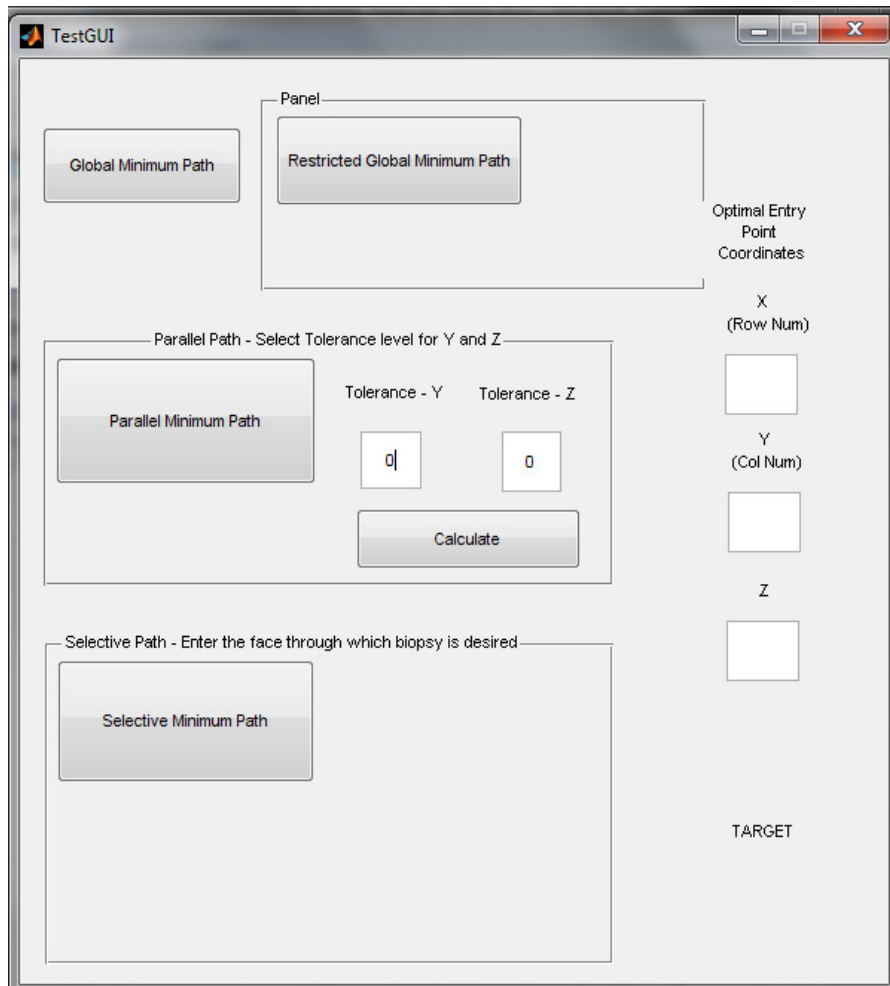


Figure 3.11 GUI for Parallel Minimum Path

The tolerances essentially act as a threshold to limit the angle of insertion of the needle in two directions, which will make sure that the doctor does not hit the chest wall/rib cage even by mistake. Based on these inputs, the contour points that lie in the specific slices within the tolerance level are considered and paths are computed for those points. The entry point of these paths must lie within the tolerance band. Paths are then filtered based on this condition; and the path with minimum cost is determined to be the best path.

2. Experienced interventional radiologists intuitively know what exactly needs to be done in order to get to the target and have developed the complex hand-eye co-ordination to

perform this task. We allow them to choose the side of the breast they wish to insert the needle, and also give them a view of that particular side that they asked for. As shown in Figure 3.7, an image will not be visible except on the first slice. We will be able to see only a black image when we display any of the other faces. Therefore, we provide slices of the image at different angles for the left and right sides, and project the curved top of the Ultrasound image onto the top and bottom (figure 3.13).

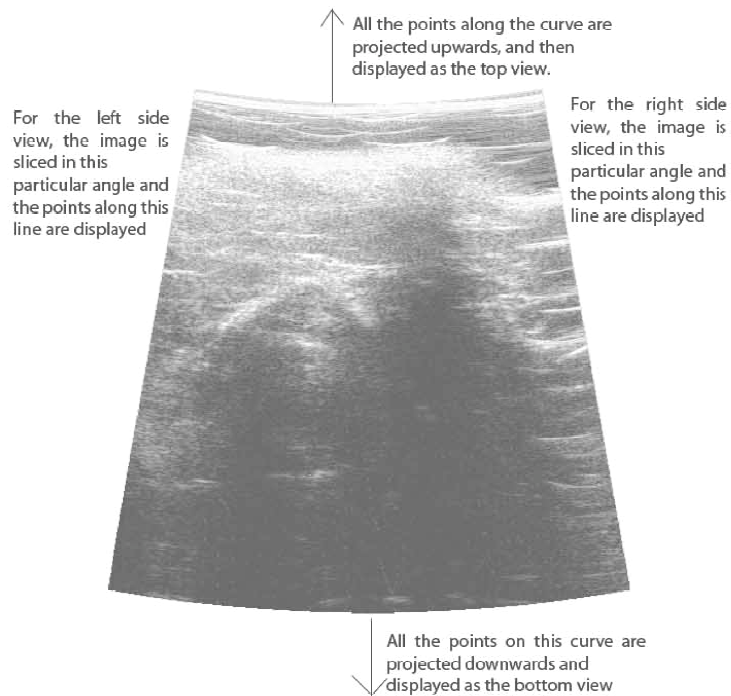


Figure 3.12 Projections for the different faces of the 3D Ultrasound

3. From this image, the doctor is made to choose 4 points that form a quadrilateral. These points are then extrapolated to get the exact points on the surface of the breast. We now have a region within which the optimal entry point lies. We enclose that region using the smallest rectangle and scan the points within that rectangle alone. Each point is checked to lie within that quadrilateral. This is done using the inpolygon function in Matlab. For all the points within the selected region, we consider them to be the entry

points and compute a path and also a weight for each path. From this set of paths, we compute the path with least cost and estimate the corresponding coordinates.

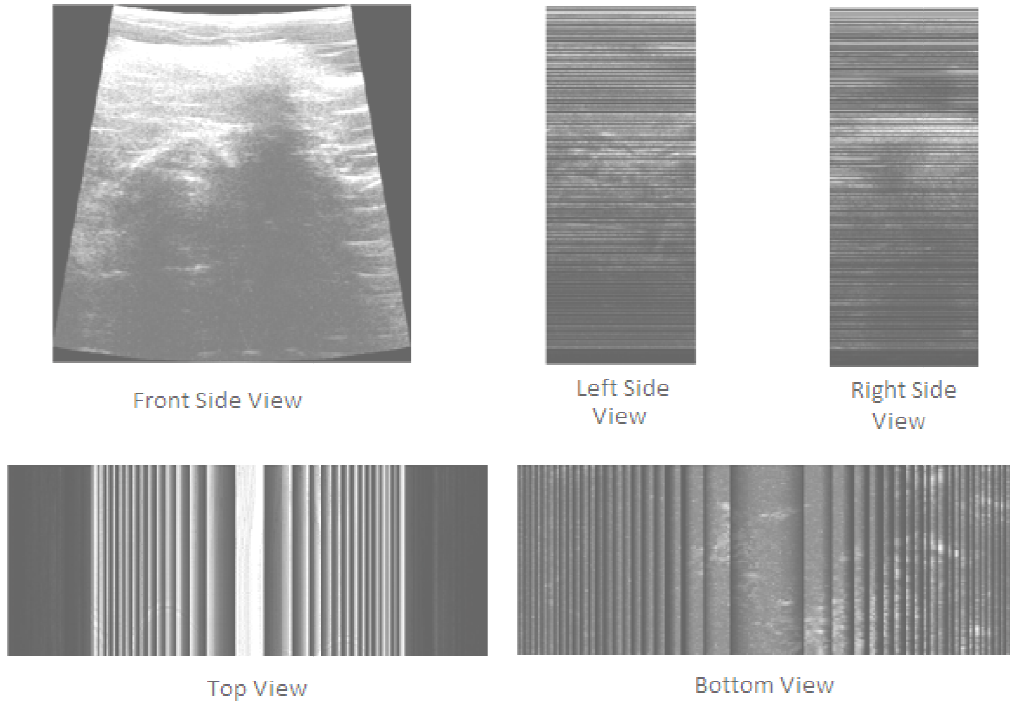


Figure 3.13 Ultrasound views of the different faces

## CHAPTER 4

### USER INTERFACE AND RESULTS

#### 4.1 User Interface

Since the Optimal Path Planning (OPP) algorithm is designed for three different levels of doctors, a simple graphical user interface (GUI) was built using Matlab (figure 4.1). It has a sub block for the three categories previously mentioned. For the first sub block, which is a global minimal path calculation, we do not require any extra inputs and it will calculate the minimal path and return the coordinates for the entry point. For the second category, a parallel path is desired. This needs inputs of the tolerance levels, for which two text boxes are given. When the values are entered, the optimal path is returned with the display showing the location of the optimal entry point. For the third category, the doctor needs to provide just the face number that he wishes to enter from. It takes values from 1 through 5, each representing a distinct face. The image of that particular face is then shown, where the doctor chooses the four points. The optimal path is then returned with the coordinates of the entry point. Screenshots of the GUI along with stages of its working are shown below.



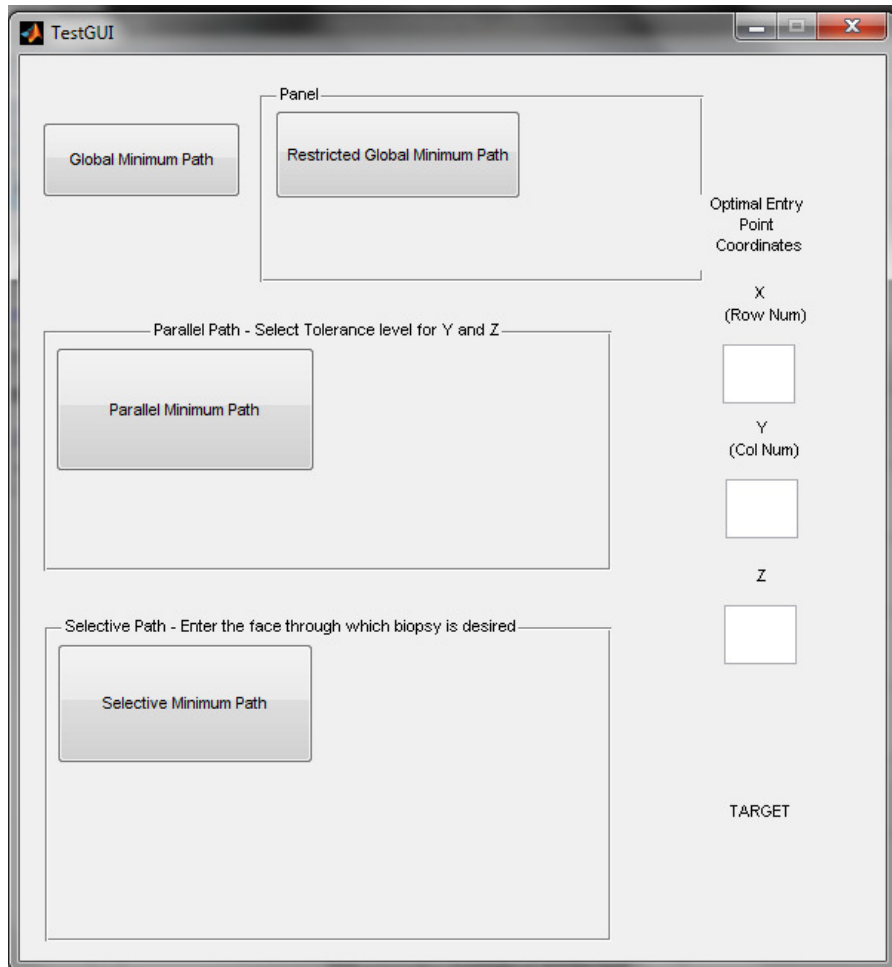


Figure 4.1 User interface

#### 4.2 Visualization

In path planning, one can verify the validity of a path only if it is seen and compared with the various other possible paths. For this purpose, a set of images were displayed which consisted of different perspectives of the same path; one is a projection of the path onto the first slice of the ultrasound image, and the other is a 3D model of the entire array in which the paths are highlighted. In the first image, we show the first slice of the ultrasound image, the zones of exclusion (if any) in red color, and the various possible paths are shown in yellow color. The best possible path is highlighted in green. For the parallel minimum path, this is feasible as the number of paths considered is not very high. For the global minimum path, the number of paths

is very high (approx 15000), which results in an image in which not much is perceived very well. Therefore, the top 25 paths which have minimum weight are shown in yellow color, and the least cost path is highlighted in green.

The second figure shows the outline of a cube that is a projection of the 3D array from a different viewing angle. From this view, we will be able to view the edges of the cube, the zones of exclusion in red color, and also the paths which were shown in the first view. These paths will be better viewed in 3D along with the optimal entry points. The doctor will be able to get a better picture of the biopsy. In order to get this 3D view, we used a function in Matlab called **viewmtx**. This function computes a 4-by-4 orthographic or perspective transformation matrix that projects four-dimensional homogeneous vectors onto a two-dimensional view surface. It takes in values as azimuth and elevation angles and returns the matrix. When the 3D world coordinates are multiplied by this matrix, they are converted to points on a 2D screen at exactly those specified angles. This results in a 3D view on a 2D screen.

### 4.3 Results

To display the results of the algorithm, we have used the user interface along with a 3D model of the ultrasound array which is displayed along with the zones of exclusion and the possible paths taken from the surface of the breast to the target tissue. We will consider different circumstances under which this algorithm was put to test and show some screenshots that were captured during simulation.

#### *4.3.1 Global Minimum Path with Zones of exclusion*

In this simulation, we compute an overall minimum path which can have any point of entry except from the bottom (since the breast cannot be entered from the bottom). Figure 4.2 shows the User interface that gives the coordinate location of the target and the optimal entry point coordinates. The visualization of the path is shown in figures 4.3 and 4.4.

For this simulation, the target and zones of exclusion were assumed to be random, and the best path is determined. The simulation results show only the top 50 candidate paths, and from them, the best possible path is shown in green, along with the optimal entry points.

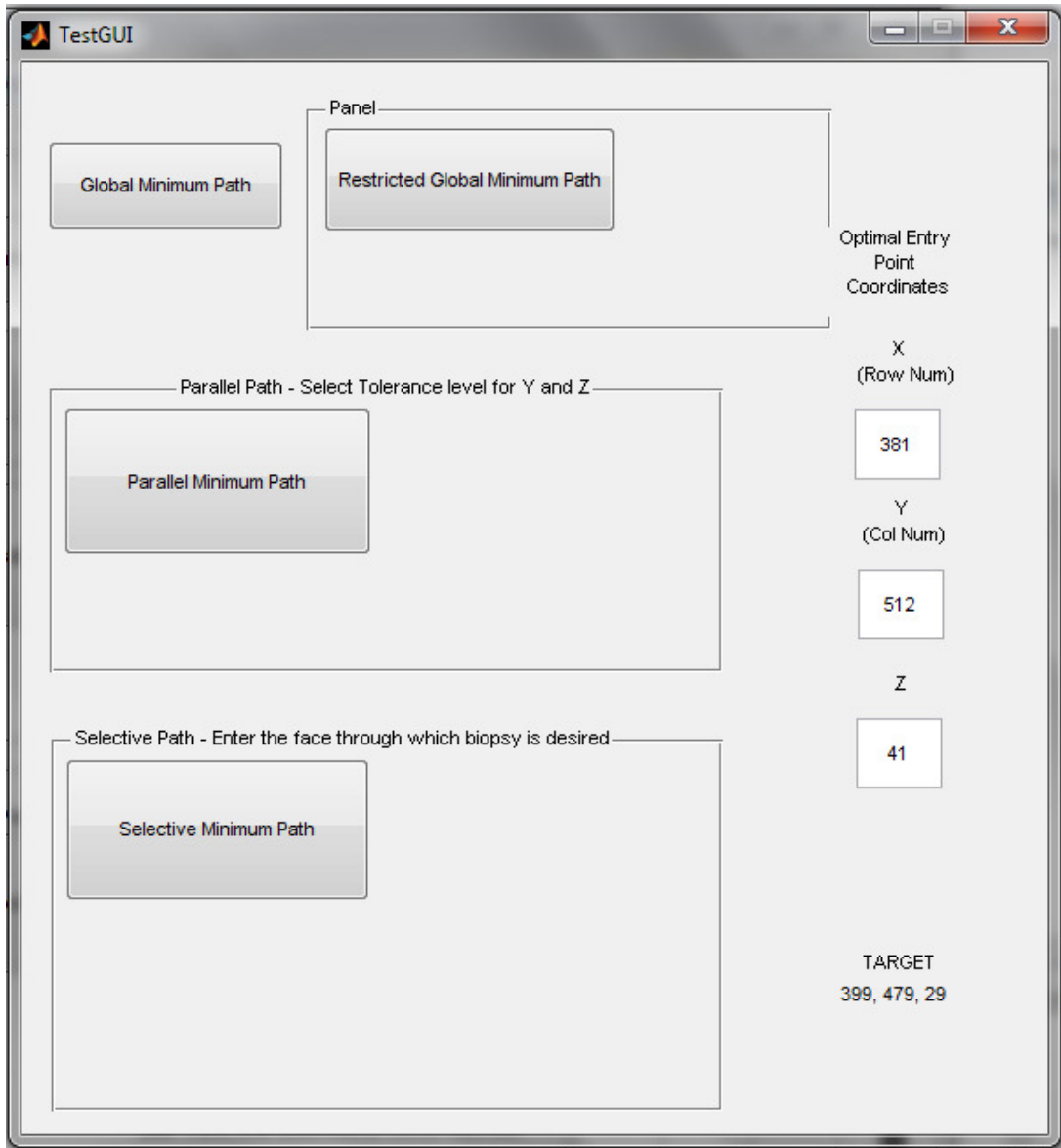


Figure 4.2 User interface for global minimum path

Figure 4.3 shows one possible 3D to 2D projection of the ultrasound array. In this figure, the top of the ultrasound and the zones of exclusion are marked. The paths from the surface to the target are shown in black lines. For better visualization, we have shown only the top 50 candidates. The most optimal path for biopsy is shown in green.

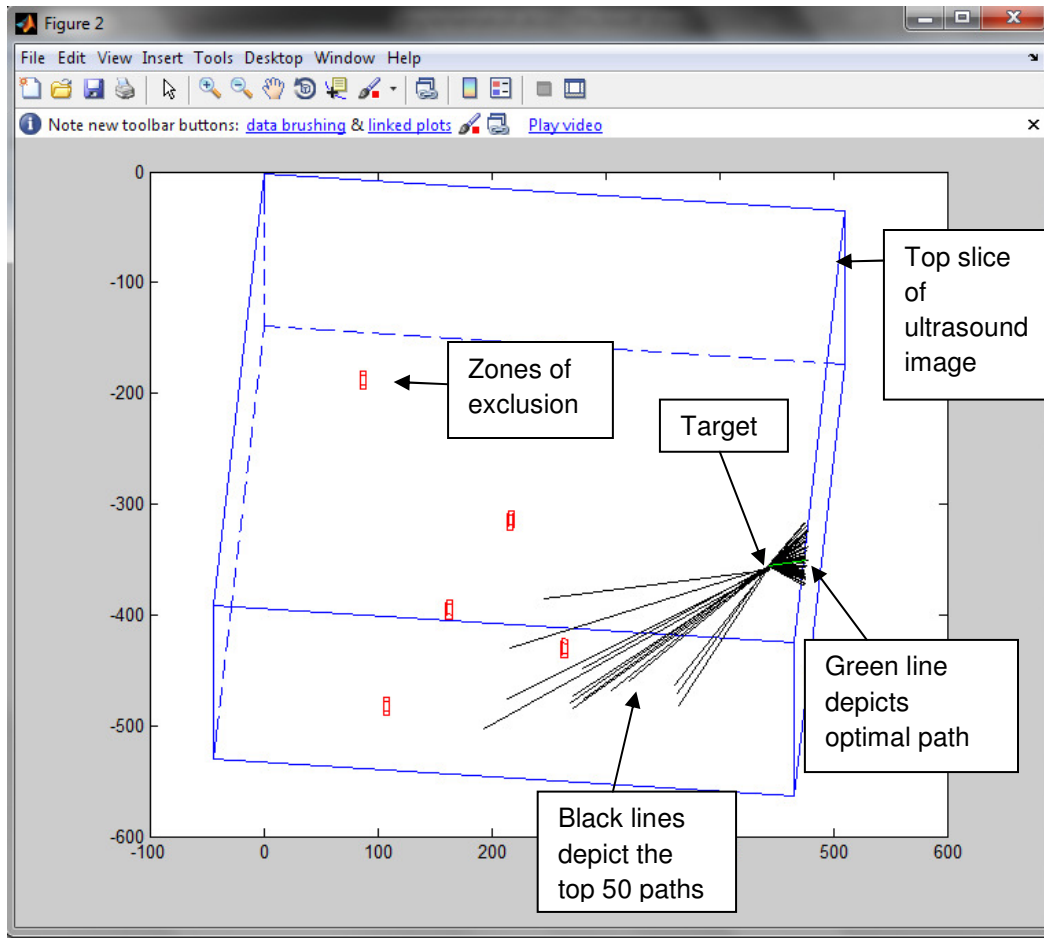


Figure 4.3 3D projection of global minimum path

This figure shows the projection of all the paths onto the front face of the ultrasound image. The yellow lines are the top 50 candidate paths with the least cost. The optimal path is shown in green.

During biopsy from certain directions, the needle moves perpendicular to the rib cage, which sometimes could risk the puncturing the chest wall if the doctor is not very careful. In order to avoid that, we consider a case where the global path is restricted to a specific band of the ultrasound image, which will be parallel to the rib cage.

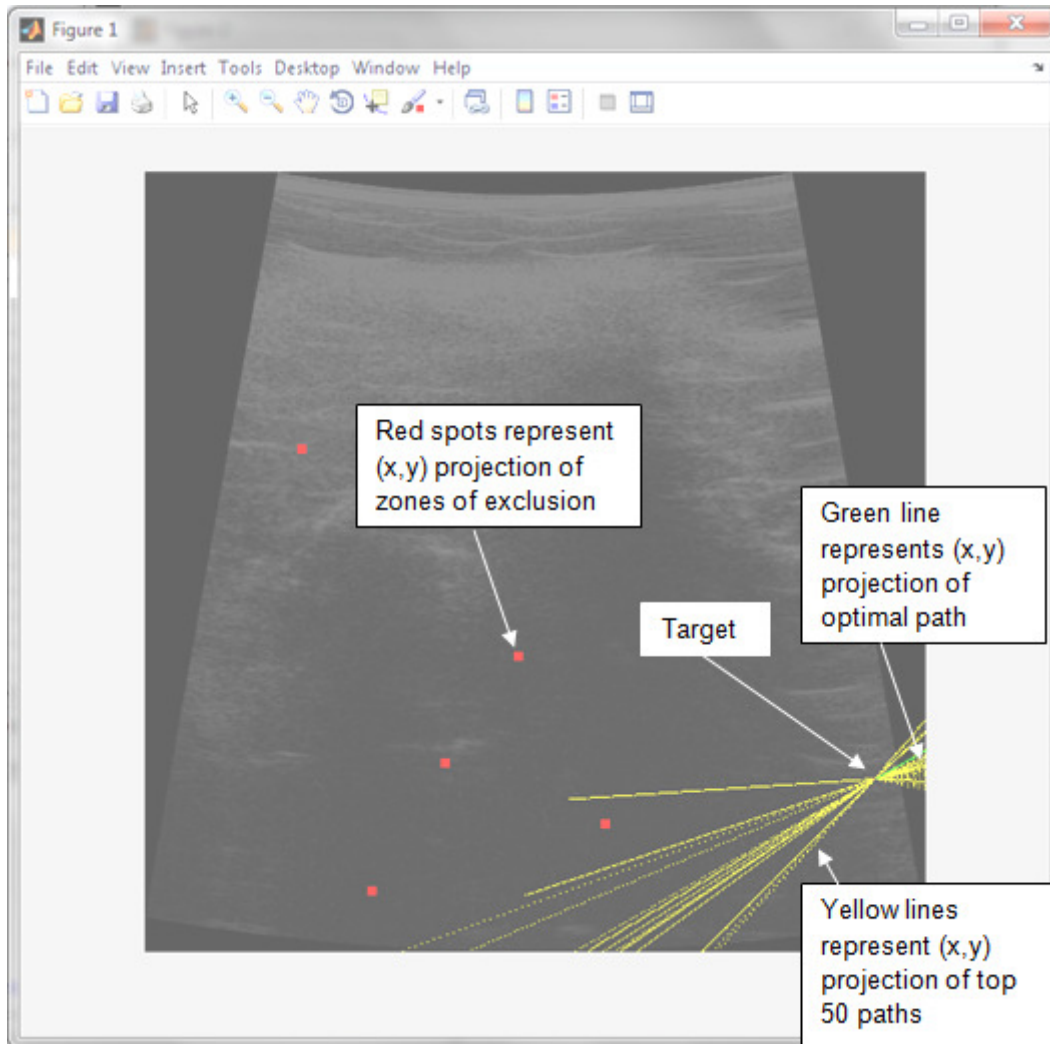


Figure 4.4 2D projections onto first Ultrasound slice for global minimum path

#### 4.3.2 Restricted Global Minimum Path with zones of exclusion

In this simulation, the target and zones of exclusion are assumed to be random and all the paths that are considered are shown in black/yellow, and the optimal path among those is shown in green.

Figure 4.5 shows the User interface panel for the Restrictive Global path method. The tolerance level in the Z direction is set to a value of 10% and all paths that have entry points within those Z values are considered.

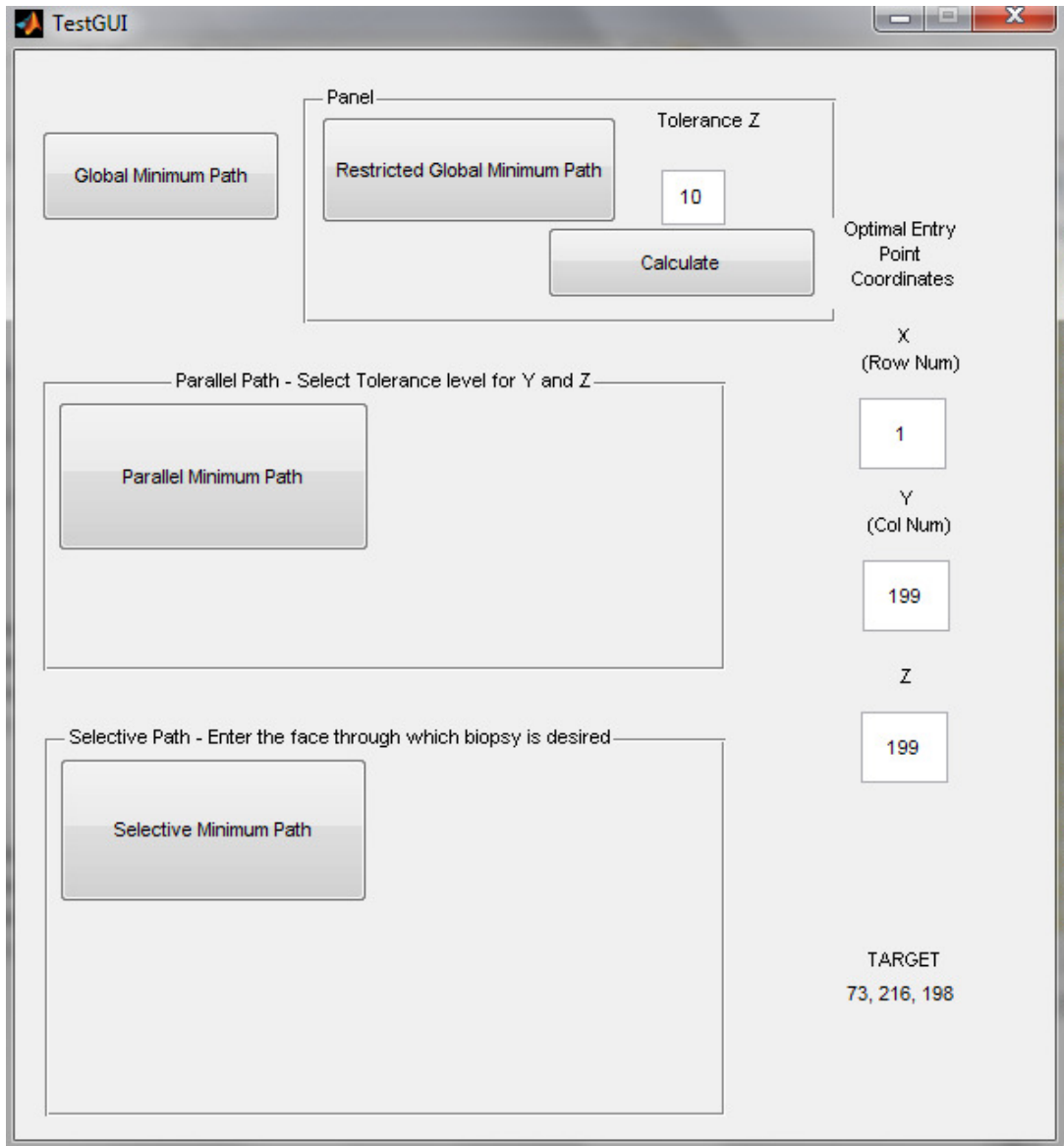


Figure 4.5 User interface for Restrictive Global Minimum path

This figure shows the top 50 candidate paths with minimum cost within the 10% tolerance that are parallel to the rib cage. We observe that the target is located in the 198<sup>th</sup> slice of the ultrasound image. The tolerance level will calculate entry points that are 5% on either side of the target. The most optimal path is indicated in green color. We see that the paths that are very close to the zones of exclusion are avoided.

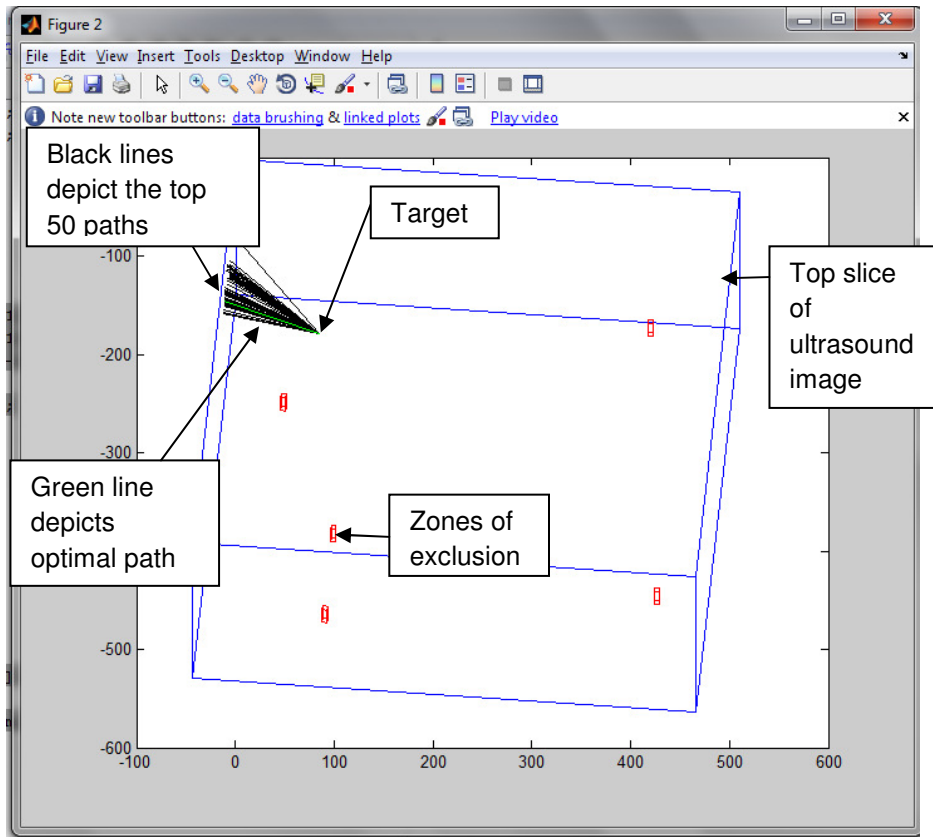


Figure 4.6 3D projections of possible paths in Restrictive Global Method

Figure 4.7 shows the top 50 paths that have minimum weights in yellow. The most optimal path is shown in green color.

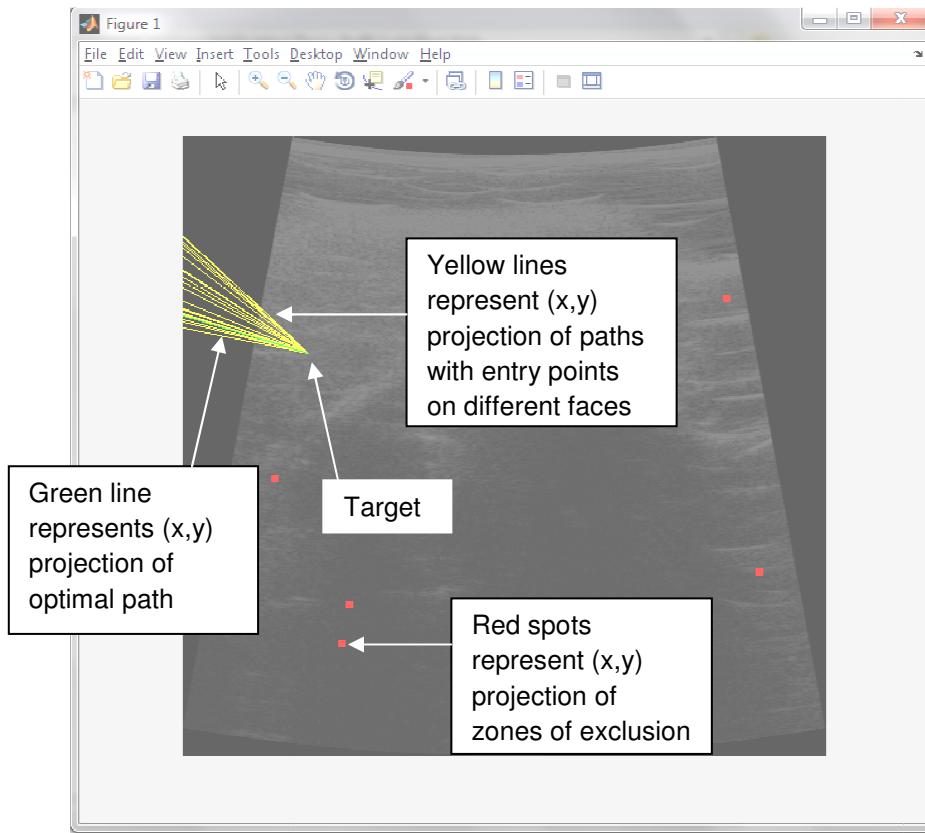


Figure 4.7 Projection of paths in Restrictive Global Method

#### 4.3.3 Parallel Minimum Path with Zones of exclusion for different angles of insertion

In order to further minimize the possibility of puncturing the chest wall, the doctor can give two tolerance levels which will totally restrict the points of entry to only the two sides of the breast. This almost ensures that the insertion can never hit the chest wall in any way.

This simulation was carried out for different tolerance levels (5, 10 and 20) and all the paths are shown, along with the optimal path in green. The target and zones of exclusion were randomly assigned. The optimal entry point coordinates are shown.

Figure 4.8 shows the user interface, where the doctor enters the tolerance levels for the paths in the X and Z coordinates are specified. The entry points that lie within this tolerance are only considered for the biopsy.



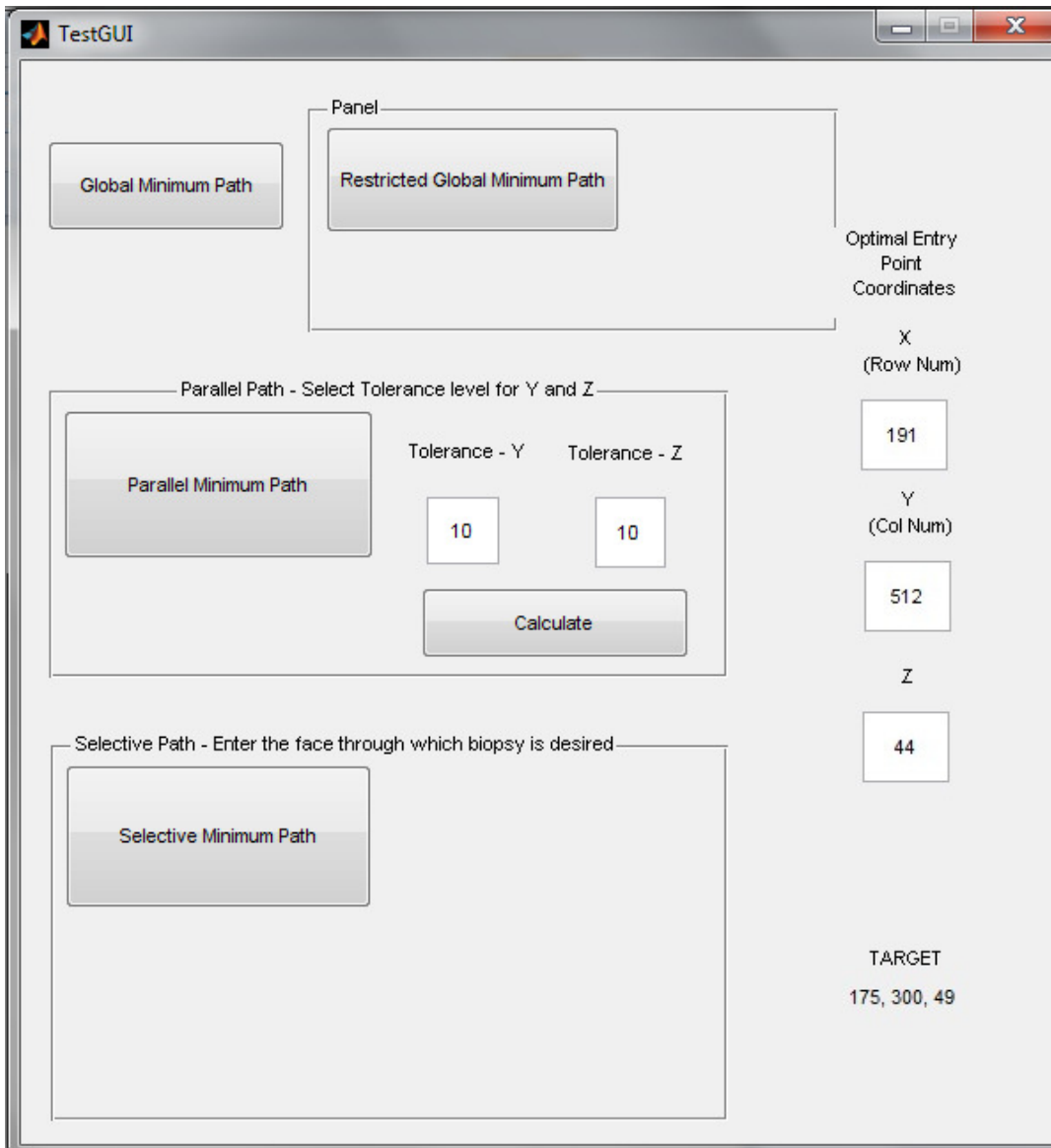


Figure 4.8 User interface for Parallel Minimum path

Figure 4.9 shows the 3D projection of all the possible parallel paths from the sides of the breast to the target tissue. The optimal path is shown in green.

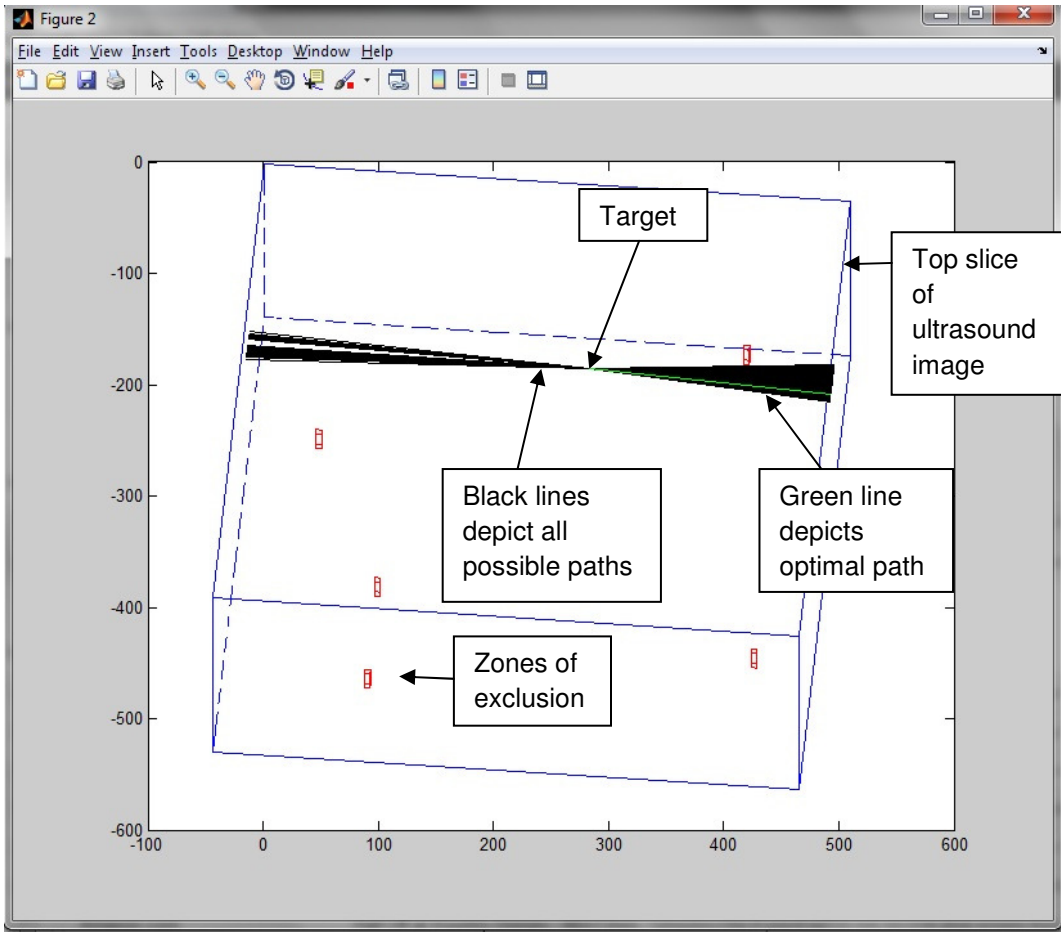


Figure 4.9 3D projections of possible paths for Parallel Minimum path

In figure 4.10, the paths are projected onto the first slice of the ultrasound image. All possible paths are shown in yellow and the optimal path which is to be followed is shown in green.

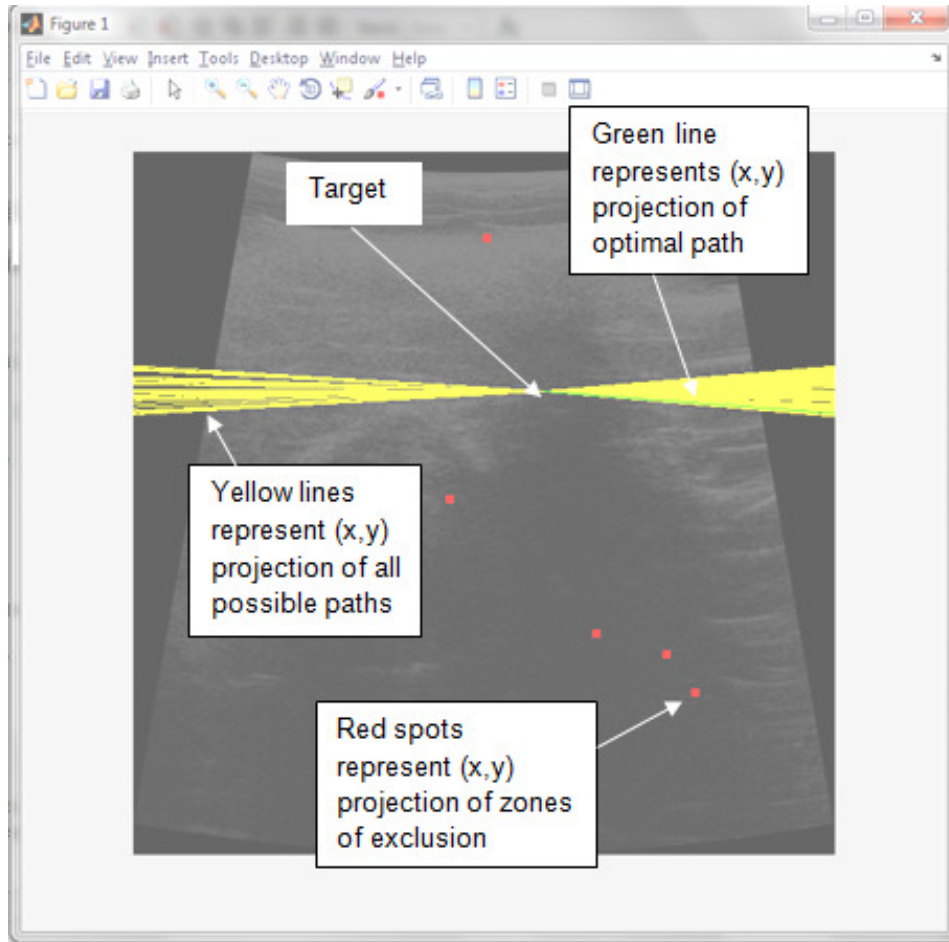


Figure 4.10 Projection of all possible paths onto first Ultrasound slice for Parallel Minimum path

#### 4.3.4 Selective Minimum Path with Zones of Exclusion

In this simulation, we allow the doctor to select the face of the surgery and the entry points, which is specified as a quadrilateral. Points inside that quadrilateral are considered as possible entry points and the best point from within that is returned. The target and zones of exclusion are randomly generated.

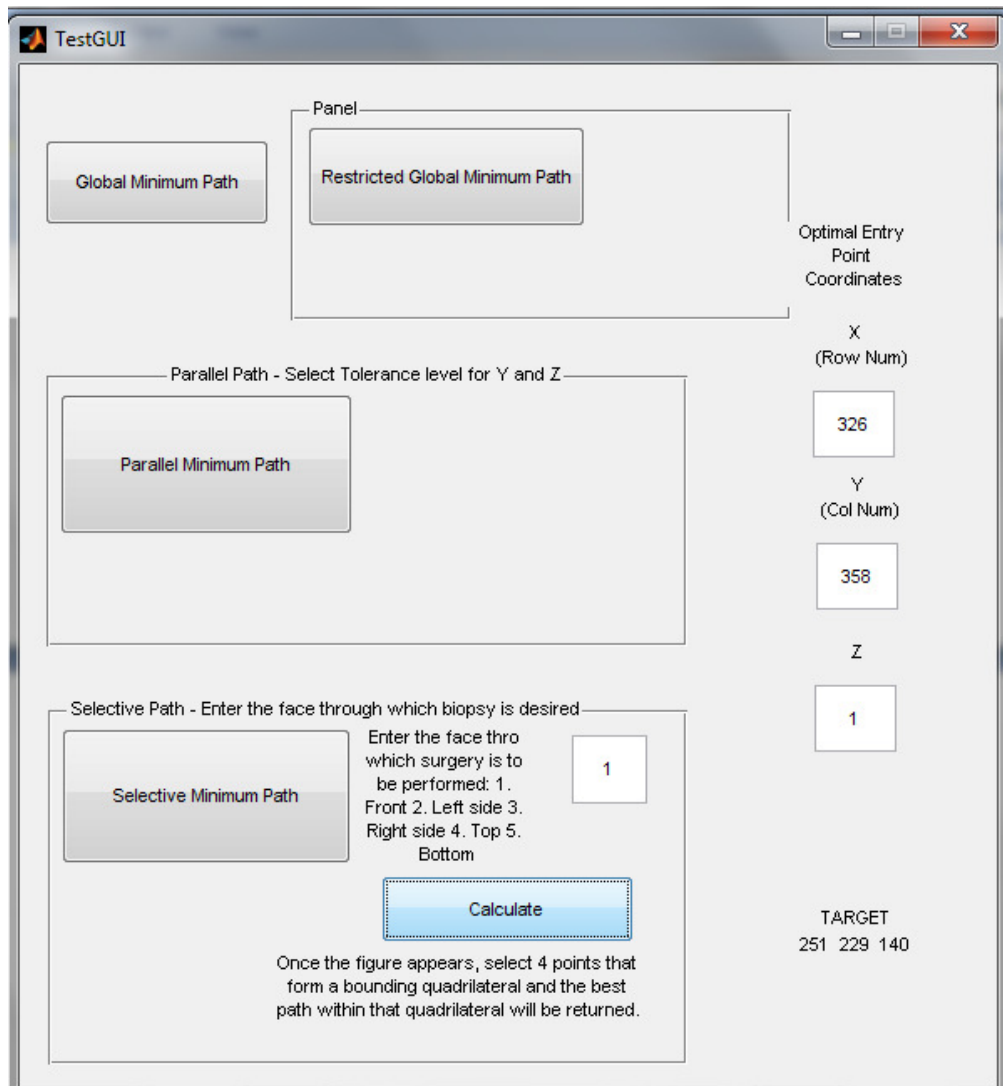


Figure 4.11 User Interface for Selective Minimum Path

Figure 4.12 shows the Ultrasound image corresponding to the face number entered by the doctor. The doctor then chooses 4 points that bound and become the region which contains the entry points. The weights are calculated only for points in this region.

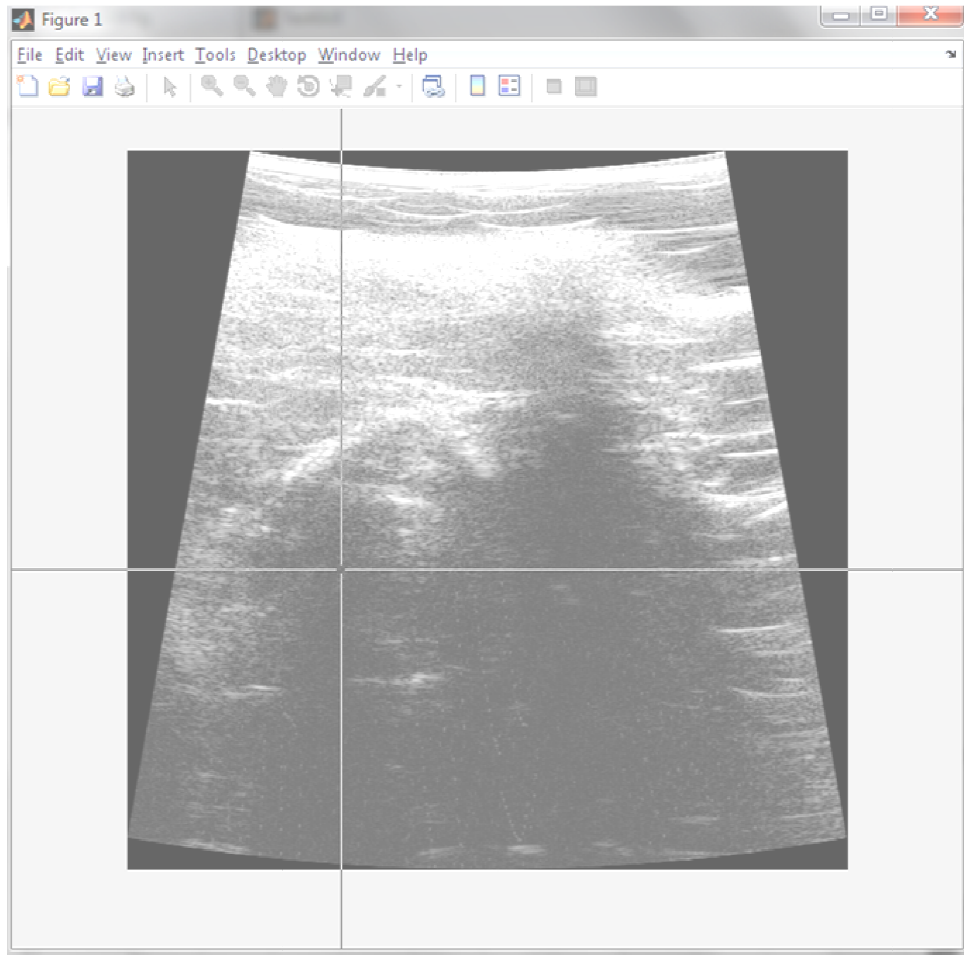


Figure 4.12 Selecting Quadrilateral from Ultrasound Image

Figure 4.13 shows all possible paths within the selected quadrilateral in black, and the optimal path is shown in green color. The zones of exclusion are indicated in red color and the top of the ultrasound slice is marked.

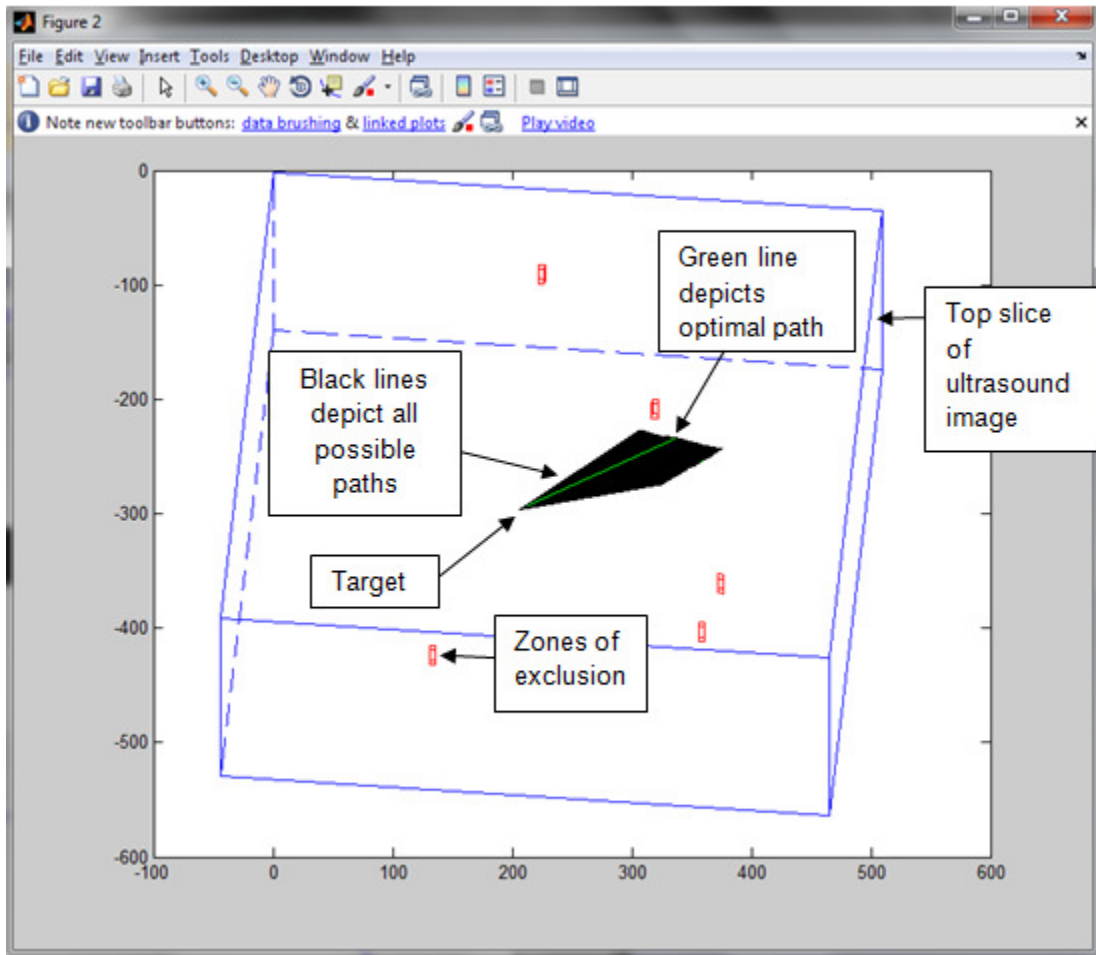


Figure 4.13 3D projections of all paths in Selective Minimum Path Method

Figure 4.14 shows the 2D projection of all the paths onto the first slice of the ultrasound image. All the possible paths from the entry point region to the target are shown in yellow, and the optimal path is shown in green.

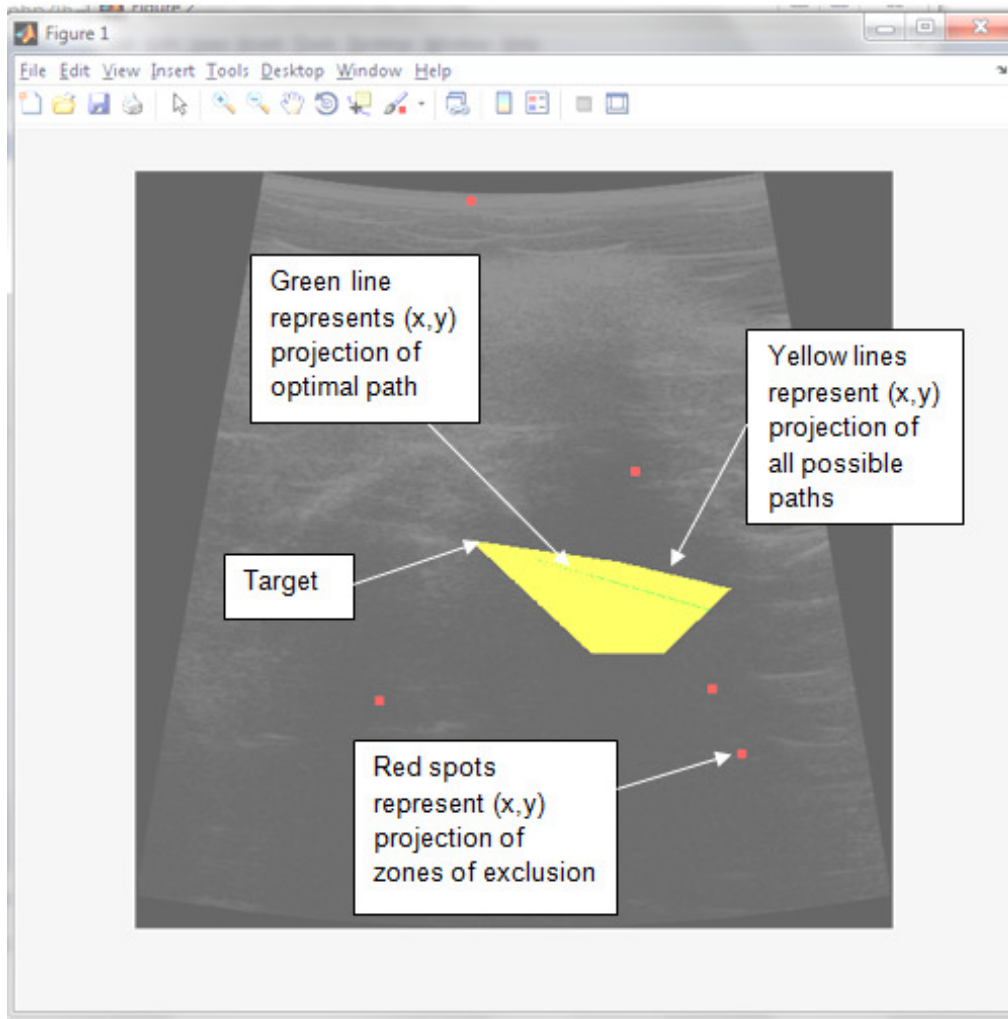


Figure 4.14 Projection onto first Ultrasound Slice for Selective Minimum Path

We have shown results of simulation of different scenarios. We conclude that the algorithm computes an optimal entry point for every case and it is compared with other paths. The optimal path clearly avoids the zones of exclusion in every case and its entry points on the surface of the breast are returned. This will be the input to the graphics block of the overall system, which will then illustrate a path from the entry point to the target, which can be viewed from any angle by the use of a 6-DOF haptic device.

Table 4.1 shows a comparison for different values of quantization levels, different threshold values and the running time of the algorithm for the simulations described in this chapter.

Table 4.1 Comparison of running time and least cost for different quantization levels and threshold values

| Target       | Algorithm                                       | Quantization | Least Cost     | Running Time | Threshold |
|--------------|---|--------------|----------------|--------------|-----------|
| [73,216,198] | Global Minimum Path                             | 8            | 8904           | 530 sec      | 75%       |
| [73,216,198] | Restrictive Global Minimum Path (Tolerance 10%) | 8            | 8904           | 503 sec      | 75%       |
| [73,216,198] | Parallel Minimum Path (Tolerances 10% each)     | 8            | 17587          | 428 sec      | 75%       |
| [73,216,198] | Global Minimum Path                             | 8            | 8966           | 363 sec      | 90%       |
| [73,216,198] | Restrictive Global Minimum Path (Tolerance 10%) | 8            | 8966           | 358 sec      | 90%       |
| [73,216,198] | Parallel Minimum Path (Tolerances 10% each)     | 8            | 17929          | 354 sec      | 90%       |
| [73,216,198] | Global Minimum Path                             | 16           | 8966           | 365 sec      | 75%       |
| [73,216,198] | Restrictive Global Minimum Path (Tolerance 10%) | 16           | 8966           | 358 sec      | 75%       |
| [73,216,198] | Parallel Minimum Path (Tolerances 10% each)     | 16           | 18574          | 348 sec      | 75%       |
| [73,216,198] | Global Minimum Path                             | 16           | 8966           | 364 sec      | 90%       |
| [73,216,198] | Restrictive Global Minimum Path (Tolerance 10%) | 16           | 8966           | 352 sec      | 90%       |
| [73,216,198] | Parallel Minimum Path (Tolerances 10% each)     | 16           | No paths found | 344 sec      | 90%       |

From this table, we can come to a conclusion that the threshold is a factor that acts as a tradeoff between the accuracy required and the running time.



## CHAPTER 5

### CONCLUSION AND FUTURE WORK

#### 5.1 Conclusion

In this thesis, we have described a potential system design which would help doctors in performing biopsy and increase accuracy of the procedure. As a part of this system, we implemented a path planning algorithm which would calculate the best possible path that takes the doctor from the surface of the breast to the target tissue.

This path planning method incorporates the mathematics described previously for a 2D case and the algorithm was modified to suit this particular case of ultrasound guided breast biopsy. This algorithm was tested on a 3D Ultrasound image data for various conditions.

The path planning was performed for a global case, where all possible paths are considered and entry-points can be anywhere except the back face of the ultrasound image. This was modified to become a restricted global minimum path, where the entry point was limited to a certain band in the Z direction, which will essentially result in paths that are parallel to the chest wall. In order to totally eradicate the possibility of accidental chest wall puncture during biopsy, we further limited the entry-points to just the two sides of the breast. This is called Parallel Path, because it is intended for the paths to be parallel to the rib cage.

The last implementation was suited for an experienced doctor. The doctor can choose the face of entry and also limit the entry points. The best entry points within the region that he marks will then be generated.

A user interface was designed which would incorporate all these conditions. In order to give a better view of the paths, we used a 3D projection to get a 3D view of the entire volume on a 2D screen. The target, the zones of exclusion and all the paths are converted to points on a 2D space using perspective projection. This is displayed along with the paths being projected onto the first slice of the Ultrasound image. This gives a much better view of the biopsy.

The threshold value and quantization level are the tradeoff factors that are chosen. The tradeoff here is between the accuracy and the running time of the algorithm. Higher values of threshold reduce the accuracy and improve the running time of the algorithm. Quantization values more than 16 will also affect the accuracy of the OPP algorithm.

### 5.2 Future Work

Our OPP algorithm calculates straight-line paths. There is ongoing research to develop a new class of needles called bevel-tip needles. The unique property of these needles is that they are flexible and can bend with a constant radius of curvature when they come in contact with soft tissue. Once these needles are used in practice, the algorithm needs to be modified in order to calculate curved paths.

The path planning is now an independent module. For the overall system to function, we need to integrate the other components and then perform testing using haptic devices.

The processing capability of this algorithm is a cause of concern. This is mainly due to the 3D Ultrasound image which occupies much memory. Better compilers like C++ or C# could be used and advanced coding concepts could be used to reduce the running time of the algorithm and make it a real-time process.

## REFERENCES

- [1] American Cancer Society, Cancer Reference Information, September 29 2011
- [2] Yoshinobu Sato, Masahiko Nakamoto, Yasuhiro Tamaki, Toshihiko Sasama, Isao Sakita, Yoshikazu Nakajima, Morito Monden, and Shinichi Tamura, "Image Guidance of Breast Cancer Surgery Using 3-D Ultrasound Images and Augmented Reality Visualization", IEEE Transactions on Medical Imaging, Vol 17, No.5, OCTOBER 1998, Pages 681 – 693.
- [3] Frank Sauer, Ali Khamene, Benedicte Bascle, Lars Schimmang, Fabian Wenzel, and Sebastian Vogt, "Augmented Reality Visualization of Ultrasound Images: System Description, Calibration, and Features", Augmented Reality, 2001. Proceedings. IEEE and ACM International Symposium, 2001, Pages 30-39
- [4] Michael Rosenthal, Andrei State, Joohee Lee, Gentaro Hirota, Jeremy Ackerman, Kurtis Keller, Etta D. Pisano, Michael Jiroutek, Keith Muller, Henry Fuchs, "Augmented Reality Guidance for Needle Biopsies: an Initial Randomized, Controlled Trial in Phantoms", Medical Image Analysis 6 (2002), Pages 313–320
- [5] A.Fenster, K.J.M.Surry, G.R.Mills, D.B.Downey, "3d Ultrasound Guided Breast Biopsy System", Ultrasonics. Volume 42, Issues 1-9, April 2004, Pages 769-774, Proceedings of Ultrasonics International 2003
- [6] Sumit Tandon, "Design and Simulation of an Accurate Breast Biopsy System", Master's Thesis, Master's Thesis, The University of Texas at Arlington, August 2007
- [7] Anantkumar S.Patel, "Haptic Guided Visualizer", Master's Thesis, The University of Texas at Dallas, April 2011
- [8] Nidhi Khullar, "Visualization of Breast Cancer Biopsy – Needle Segmentation in Ultrasound Image", Master's Thesis, The University of Texas at Arlington, November 2011

- [9] Simon P DiMaio and S.E.Salcudean, "Needle Steering and Motion Planning in Soft Tissues", IEEE Transactions on Biomedical Engineering, June 2005, Volume 52 Issue 6, Pages 965-974
- [10] Ron Alterovitz, Michael Branicky and Ken Goldberg, "Motion Planning Under Uncertainty for Image-guided Medical Needle Steering", The International Journal of Robotics Research, November/December 2008 vol. 27 no. 11-12
- [11] Nuttapon Chentanez, Ron Alterovitz, Daniel Ritchie, Lita Cho, Kris K. Hauser, Ken Goldberg, Jonathan R. Shewchuk, and James F. O'Brien, "Interactive Simulation of Surgical Needle Insertion and Steering", Proceedings of ACM SIGGRAPH 2009, pages 88:1–10, Aug 2009.
- [12] Kris Hauser, Ron Alterovitz, Nuttapon Chentanez, Allison Okamura, and Ken Goldberg, "Feedback Control for Steering Needles Through 3D Deformable Tissue Using Helical Paths", Proceedings of Robotics: Science and Systems, June 2009
- [13] Laurence Vancamberg, Anis Sahbani, Serge Muller, and Guillaume Morel, "Needle Path Planning Method for Digital Breast Tomosynthesis Biopsy Based on Probabilistic Techniques", Digital Mammography/IWDM Proceedings, 2010
- [14] Ron Alterovitz, Kenneth Y. Goldberg, Jean Pouliot, and I-Chow (Joe) Hsu, "Sensorless Motion Planning for Medical Needle Insertion in Deformable Tissues", IEEE Transactions on Information Technology in Biomedicine, Vol 13 No 2, March 2009
- [15] Danny Z.Chen, Ovidiu Daescu, Xiaobo (Sharon) Hu, Xiaodong Wu, Jinhui Xu, "Determining an Optimal Penetration Among Weighted Regions in Two and Three Dimensions", Journal of Combinatorial Optimization, 5, 59–79, 2001
- [16] Ovidiu Daescu and James Palmer, "Minimum Separation in Weighted Subdivisions", International Journal of Computational Geometry and Applications, Vol 19 No 1 (2009) pp 33-57
- [17] Michel Pocchiola, Gert Vetger, "The Visibility Complex", SCG 1993 Proceedings of the ninth annual symposium on Computational Geometry

## BIOGRAPHICAL INFORMATION

Sridhar Rajaram was born on 12<sup>th</sup> January, 1988 in Tamilnadu, India. He completed his schooling in Padma Seshadri Bala Bhavan Senior Secondary School, Chennai, India in 2005. He then got his Bachelor's degree in Electronics and Communication Engineering from Anna University, Chennai, India in 2009. He joined The University of Texas at Arlington in August 2009 in the Electrical Engineering Department. He worked as a Graduate Research Assistant at the Virtual Environment Laboratory (VEL) from January 2010 to December 2011. He completed his Master's in Electrical Engineering in December 2011.